

On a paradox in the impact dynamics of smooth rigid bodies

Peter Palffy-Muhoray¹

Epifanio G. Virga^{2*}

Mark Wilkinson³

Xiaoyu Zheng⁴

¹Liquid Crystal Institute, Kent State University, OH, USA

²Mathematical Institute, University of Oxford, Oxford, UK

³Mathematical and Computer Sciences, Heriot-Watt University, Edinburgh, UK

⁴Department of Mathematical Sciences, Kent State University, OH, USA

January 6, 2022

Abstract

Paradoxes in the impact dynamics of rigid bodies are known to arise in the presence of friction. We show here that, on specific occasions, in the absence of friction, the conservation laws of classical mechanics are also incompatible with the collisions of smooth, strictly convex rigid bodies. Under the assumption that the impact impulse is along the normal direction to the surface at the contact point, two convex rigid bodies which are well separated can come into contact, and then interpenetrate each other. This paradox can be constructed in both 2D and 3D when the collisions are tangential, in which case no momentum or energy transfer between the two bodies is possible. The postcollisional interpenetration can be realized through the contact points or through neighboring points only. The penetration distance is shown to be $O(t^3)$. The conclusion is that rigid body dynamics is not compatible with the conservation laws of classical mechanics.

1 Introduction

As is the case with dragons [1], everyone knows that rigid bodies do not exist. Nonetheless, the study of the dynamics of rigid bodies can give valuable insights into the behavior of real compressible many-body systems. We refer to [2] for a recent, broad account of this old, but still flourishing, subject.

*On leave from Dipartimento di Matematica, Università di Pavia, Pavia, Italy

Systems of hard spheres, interacting via steric repulsion, have also received a great deal of attention in simulating soft matter systems. The *hard-sphere paradigm* is the assumption that, to a good approximation, any simple liquid with strongly repulsive forces may be modeled as a system of hard spheres. Typically, in the hard sphere paradigm, hard sphere particles have no rotational degrees of freedom, and move in straight lines with constant velocity until they collide elastically; that is, by conserving linear momentum and kinetic energy. A current review is provided in Ref. [8]. By contrast, the dynamics of systems of non-spherical hard particles have received far less attention.

The dynamics of non-spherical particles have been addressed in a recent work [3], extending the theory of the Boltzmann equation from hard spheres to general hard particles. In Ref. [3] it is suggested that it may not always be “possible to construct a family of scattering matrices corresponding to the collision of two non-spherical particles which conserves their total linear momentum, angular momentum and kinetic energy”; that is, the dynamics of non-spherical hard particles may not be fully compatible with the conservation laws of classical mechanics. The specific concern was that the dynamics prescribed by the conservation laws could, in rare instances, result in the interpenetration of the colliding bodies.

Paradoxes in the impact dynamics of rigid bodies have been known to exist for a long time. The classical balance laws of mechanics are not sufficient to solve the problem of impact between two rigid bodies, that is, to predict the motion of two colliding bodies after the impact, once their motion before impact is known. The classical balance laws must be supplemented by an additional *impact* (or *collision*) law, which is constitutive in nature and must ultimately be justified (or at least confirmed) experimentally.¹ As lucidly explained in Chapter 4 of [2], impact laws fall into three broad categories. They all relate mechanical properties of the colliding bodies before and after impact. What distinguishes the three categories is the nature of these properties: they may relate velocities, impulses, or kinetic energies. While the first two categories are classical, having already been introduced in the works of Newton and Poisson (see also [11]), the third category is rather more recent in its inception: it was introduced by Stronge [12] to overcome paradoxes that arise in the presence of friction [13, 14, 15].² These paradoxes showed instances in which Newton’s law of impact would imply an energy gain. However, as also remarked in [12], for *smooth* (frictionless)

¹Many such laws have been proposed in the past: in particular, we refer the interested reader to [4, 5], where new laws are advanced and they are also contrasted with the vast repertoire of pre-existing laws.

²Other paradoxes arise in the dynamics of colliding rigid bodies, but they pertain more to the laws of friction than to the laws of impact. Among these, we just mention the impact variant of Painlevé paradox [6, 7].

rigid bodies all three categories are equivalent and reduce to one and the same prescription, which is consistent with the conservation of linear momentum, angular momentum, and kinetic energy. The known paradoxes of impact dynamics simply evaporate as friction is neglected.

In this paper, we examine collisions of smooth, strictly-convex hard particles, and conclude that although these almost always satisfy the conservation laws without interpenetration, there may occur rare events where, remarkably, this is not the case. We conclude therefore that the dynamics of strictly-convex hard particles are, in general, *not* consistent with the conservation laws of classical mechanics. Alternatively, we could say that enforcing momentum conservation and rigidity in the instances shown here would violate energy conservation. This is the new paradox described in this paper.

The outline of the paper is as follows. Section 2 on conservation laws establishes the connection between momentum transfer and the motion of rigid bodies. Section 3 provides a simple 2D paradigm which illustrates the basis of the paradox in an elementary way. Section 4 is divided into two parts. The first part, 4.1, outlines how the surfaces of the colliding bodies are characterized, and how the distances between them are measured. The points neighboring the points of contact play an important role, and their relevant kinematics are described. The second part, 4.2, identifies specific collision scenarios, and classifies their behavior. The main result of the paper, the inconsistency of rigid body dynamics and the conservation laws of classical mechanics is demonstrated. Section 5 summarizes our results. The paper is accompanied by a Supplementary Data file. In particular, Supplementary Data I gives one exact and analytically described example in 2D, and two numerical examples of collisions in 2D and 3D illustrating the inconsistency. Supplementary Data II provides essential information on the explicit definitions of terms appearing in the main body of the paper. Supplementary Data III provides a detailed derivation of the equations of motion, while Supplementary Data IV gives proofs of assertions made in the main body of the paper.

2 Conservation laws and collision dynamics

In this section, we consider the frictionless collisions of particles which are strictly-convex rigid bodies of arbitrary but smooth shape. We assume that the closed bounding surfaces of the bodies are sufficiently smooth to allow all partial derivatives up to second order to be well defined at each point on the surface. We examine how two arbitrary but strictly-convex rigid bodies, body 1 and body 2, change their momenta upon collision.

A collision is an event when particles interact and may exchange momentum. We consider collisions where the particles are well separated before collision, and, following their trajectories, come into a single point contact and can interact with each other. The interaction is via a hard core interaction potential, which is positive infinite if the particles interpenetrate, and is zero otherwise. Since the particle energies are finite, interpenetration of one rigid body by another, where two particles have more than one point in common, is not possible. Thus, a collision is an event when two particles, which were well separated before, are in single point contact externally. Since the forces the particles exert on each other are gradients of the potential, if forces are exerted, their magnitude is infinite. Since the momenta and kinetic energies are finite, collisions are necessarily instantaneous; that is, the impulse is a delta function in time.

In elastic collisions, linear and angular momenta and kinetic energy may be exchanged, but must be conserved. Unlike compressible bodies, rigid body systems have no mechanism for dissipation, and since there is no potential energy except at the instant of the collision, kinetic energy must be conserved.

We assume that the bodies are frictionless; that is, the direction of the exchanged linear momentum is along the common normal to the two surfaces at the point of contact. If the impulse acting on body 1 is $-\alpha\hat{\mathbf{n}}_1$, where α is the magnitude of the impulse and $\hat{\mathbf{n}}_1$ is the unit outward normal at the surface of body 1 at the point of contact, then the conservation of linear momentum gives

$$m_1(\mathbf{v}_{1f} - \mathbf{v}_{1i}) = -\alpha\hat{\mathbf{n}}_1, \quad (1)$$

$$m_2(\mathbf{v}_{2f} - \mathbf{v}_{2i}) = \alpha\hat{\mathbf{n}}_1, \quad (2)$$

where m_1 and m_2 are the masses of bodies 1 and 2 with centers of mass at \mathbf{r}_{c1} and \mathbf{r}_{c2} , \mathbf{v}_{1i} and \mathbf{v}_{2i} are the pre-collision and \mathbf{v}_{1f} and \mathbf{v}_{2f} are the post-collision velocities of the centers of mass. The bodies move freely in space: in the absence of collisions, linear momentum is unchanged, and the center of mass of each body moves with constant velocity.

Conservation of angular momentum gives

$$\mathbf{I}_1(\boldsymbol{\omega}_{1f} - \boldsymbol{\omega}_{1i}) = -\alpha\mathbf{p} \times \hat{\mathbf{n}}_1, \quad (3)$$

$$\mathbf{I}_2(\boldsymbol{\omega}_{2f} - \boldsymbol{\omega}_{2i}) = \alpha\mathbf{q} \times \hat{\mathbf{n}}_1, \quad (4)$$

where \mathbf{I}_1 and \mathbf{I}_2 are the moment of inertia tensors of bodies 1 and 2 about their centers of mass, $\boldsymbol{\omega}_{1i}$ and $\boldsymbol{\omega}_{2i}$ are pre-collision and $\boldsymbol{\omega}_{1f}$ and $\boldsymbol{\omega}_{2f}$ are post-collision angular velocities. The vector \mathbf{p}

is a body-fixed vector from the center of mass of body 1 to the point P in body 1 which is the contact point at the instant of collision, and \mathbf{q} is a body-fixed vector from center of mass of body 2 to the point Q in body 2 which is the contact point at the instant of collision. (We shall refer to the points P and Q in general as contact points, even though they are only in contact with each other at the instant of collision.)

We note that in the absence of collisions, angular momentum about the center of mass is unchanged. However, since in general the moment of inertia is changing due to rotation, the angular velocity also changes in time. The angular acceleration in an inertial reference frame is

$$\dot{\boldsymbol{\omega}} = -\mathbf{I}^{-1} \cdot (\boldsymbol{\omega} \times (\mathbf{I} \cdot \boldsymbol{\omega})), \quad (5)$$

in accordance with Euler's equations [9].

Finally, the conservation of kinetic energy requires that

$$\begin{aligned} & \frac{1}{2}m_1\mathbf{v}_{1i}^2 + \frac{1}{2}m_2\mathbf{v}_{2i}^2 + \frac{1}{2}\boldsymbol{\omega}_{1i} \cdot \mathbf{I}_1 \cdot \boldsymbol{\omega}_{1i} + \frac{1}{2}\boldsymbol{\omega}_{2i} \cdot \mathbf{I}_2 \cdot \boldsymbol{\omega}_{2i} \\ = & \frac{1}{2}m_1\mathbf{v}_{1f}^2 + \frac{1}{2}m_2\mathbf{v}_{2f}^2 + \frac{1}{2}\boldsymbol{\omega}_{1f} \cdot \mathbf{I}_1 \cdot \boldsymbol{\omega}_{1f} + \frac{1}{2}\boldsymbol{\omega}_{2f} \cdot \mathbf{I}_2 \cdot \boldsymbol{\omega}_{2f}. \end{aligned} \quad (6)$$

We note that $\mathbf{v}_{Pi} = \mathbf{v}_{1i} + \boldsymbol{\omega}_{1i} \times \mathbf{p}$ and $\mathbf{v}_{Qi} = \mathbf{v}_{2i} + \boldsymbol{\omega}_{2i} \times \mathbf{q}$ are the pre-collision and $\mathbf{v}_{Pf} = \mathbf{v}_{1f} + \boldsymbol{\omega}_{1f} \times \mathbf{p}$ and $\mathbf{v}_{Qf} = \mathbf{v}_{2f} + \boldsymbol{\omega}_{2f} \times \mathbf{q}$ are the post-collision velocities of the contact points P and Q on bodies 1 and 2. Solving for α , we find two solutions. One solution is $\alpha = 0$, corresponding to no momentum or energy transfer. The second solution is given by

$$\alpha = 2 \frac{(\mathbf{v}_{Pi} - \mathbf{v}_{Qi}) \cdot \hat{\mathbf{n}}_1}{\hat{\mathbf{n}}_1 \cdot \mathbf{M} \cdot \hat{\mathbf{n}}_1}, \quad (7)$$

where

$$\mathbf{M} = \left(\frac{1}{m_1} + \frac{1}{m_2} \right) \mathbb{I} - \mathbf{p} \times \mathbf{I}_1^{-1} \times \mathbf{p} - \mathbf{q} \times \mathbf{I}_2^{-1} \times \mathbf{q}, \quad (8)$$

and \mathbb{I} is the identity tensor.³ The cross-products are of the vectors and the eigenvectors of the tensors in their canonical form. Eq. (7) implies that the magnitude of the impulse, and of the exchanged momenta, is proportional to the normal velocity of approach of the contact points.

The velocity of separation is given by

$$\mathbf{v}_{Pf} - \mathbf{v}_{Qf} = (\mathbf{v}_{Pi} - \mathbf{v}_{Qi}) \cdot \left[\mathbb{I} - 2\hat{\mathbf{n}}_1\hat{\mathbf{n}}_1 \cdot \frac{\mathbf{M}}{\hat{\mathbf{n}}_1 \cdot \mathbf{M} \cdot \hat{\mathbf{n}}_1} \right]. \quad (9)$$

³The product $\mathbf{a} \times \mathbf{B} \times \mathbf{c}$, where \mathbf{a} and \mathbf{c} are vectors, and \mathbf{B} is a tensor, is a tensor with Cartesian components $\varepsilon_{\alpha\beta\gamma}a_\beta B_{\gamma\delta}\varepsilon_{\mu\delta\nu}c_\nu$, where $\varepsilon_{\alpha\beta\gamma}$ is the Levi-Civita symbol.

It follows at once that

$$(\mathbf{v}_{Pf} - \mathbf{v}_{Qf}) \cdot \hat{\mathbf{n}}_1 = -(\mathbf{v}_{Pi} - \mathbf{v}_{Qi}) \cdot \hat{\mathbf{n}}_1, \quad (10)$$

in agreement with [10]. That is, the post-collision speed of separation of the contact points along the normal is equal to their pre-collision speed of approach along the normal. This result is essential to our arguments below.

We note that if the collision were not instantaneous, then during the collision the speed of separation would, for some instants of time, differ from the final speed of separation [16]. This would clearly violate energy conservation, since, unlike in the case of interactions via soft potentials, energy cannot be stored as potential energy. Rigid body collisions must, again, therefore be instantaneous.

In what follows, we distinguish two types of collisions.

In the first type, which we call ‘normal’ collisions, the two particles approach each other with a non-zero normal velocity of approach of the contact points; here we note that $\alpha \neq 0$. In this case, there is instantaneous momentum transfer, with the magnitude indicated in Eq. (7), and, in general, there is also energy transfer between the particles.

In the second type, which we call ‘tangential’ collisions, the contact points approach each other along the tangent to the surfaces at the points of contact, and in this way come into contact with each other. Here $\alpha = 0$, and in this case, there is neither momentum nor energy transfer.

3 A 2D Paradigm

To gain some initial insight into the collisions under study, we consider, as an illustrative example, the tangential collision of an ellipse with an irregular convex body, shown in Fig. 1.

The collision occurs at time $t = 0$, the point of collision on body 1 is P and on body 2 it is Q . The x -axis coincides with the common tangent line at the contact points of the two bodies. For simplicity, we assume that body 1 is at rest. At time $t = 0$, the center of mass M of body 2 is at position \mathbf{r}_M , moving with constant velocity \mathbf{v}_M . Body 2 is also rotating with angular velocity $\boldsymbol{\omega}$, normal to the plane of the bodies. The radius of curvature of body 2 at the point of contact is R_0 , the center of curvature C is at position \mathbf{r}_C . We define $\hat{\mathbf{x}}$ and $\hat{\mathbf{y}}$ as unit vectors along the x - and y -axes, respectively.

The velocity \mathbf{v}_Q of the point of contact Q is given by⁴

$$\mathbf{v}_Q = \mathbf{v}_M - \boldsymbol{\omega} \times \mathbf{r}_M. \quad (11)$$

⁴For convenience, we use the 3D vector product here, although both bodies are in 2D.

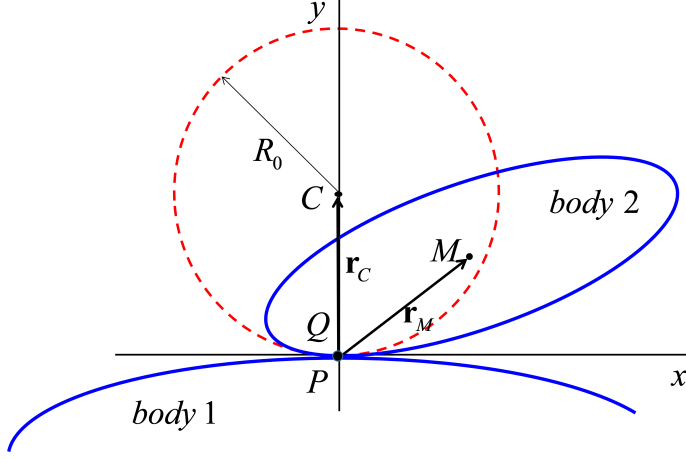


Figure 1: Collision of two convex bodies in 2D. Body 2 with center of mass M at \mathbf{r}_M , translating with constant velocity \mathbf{v}_M and rotating with constant angular velocity $\boldsymbol{\omega}$ comes into contact at the origin with body 1 at rest. The radius of curvature for body 2 at the contact point Q is R_0 , and the center of curvature C is at position \mathbf{r}_C .

If the collision is tangential, then $\mathbf{v}_Q \cdot \hat{\mathbf{y}} = 0$, and we must have

$$\mathbf{v}_M \cdot \hat{\mathbf{y}} = \boldsymbol{\omega} \times \mathbf{r}_M \cdot \hat{\mathbf{y}}, \quad (12)$$

but $\mathbf{v}_M \cdot \hat{\mathbf{x}}$ is arbitrary. The acceleration \mathbf{a}_Q of the point of contact Q is given by

$$\mathbf{a}_Q = \omega^2 \mathbf{r}_M, \quad (13)$$

and its normal acceleration is

$$\mathbf{a}_Q \cdot \hat{\mathbf{y}} = \omega^2 \mathbf{r}_M \cdot \hat{\mathbf{y}}. \quad (14)$$

Since the relative normal velocity of the colliding bodies is zero, there is no momentum transfer, hence body 1 remains at rest, and the motion of body 2 is unchanged after the collision.

It is interesting to consider the motion of the center of curvature C and of the circular arc near P along the normal $\hat{\mathbf{y}}$. In general, the vertical position of C can be written, for small t , as

$$\mathbf{r}_C(t) \cdot \hat{\mathbf{y}} = R + \mathbf{v}_C \cdot \hat{\mathbf{y}}t + \frac{1}{2}\mathbf{a}_C \cdot \hat{\mathbf{y}}t^2 + \frac{1}{6}\mathbf{j}_C \cdot \hat{\mathbf{y}}t^3 + O(t^4), \quad (15)$$

where \mathbf{v}_C is the velocity, \mathbf{a}_C is the acceleration, and \mathbf{j}_C is the jerk of C . The velocity \mathbf{v}_C of C along the normal is

$$\mathbf{v}_C \cdot \hat{\mathbf{y}} = \mathbf{v}_M \cdot \hat{\mathbf{y}} + (\boldsymbol{\omega} \times (\mathbf{r}_C - \mathbf{r}_M)) \cdot \hat{\mathbf{y}}, \quad (16)$$

which, due to the choice of \mathbf{v}_M , is

$$\mathbf{v}_C \cdot \hat{\mathbf{y}} = (\boldsymbol{\omega} \times \mathbf{r}_C) \cdot \hat{\mathbf{y}} = 0. \quad (17)$$

The acceleration of C along the normal is

$$\mathbf{a}_C \cdot \hat{\mathbf{y}} = -\omega^2 (\mathbf{r}_C - \mathbf{r}_M) \cdot \hat{\mathbf{y}}, \quad (18)$$

which vanishes in the special case when

$$\mathbf{r}_C \cdot \hat{\mathbf{y}} = \mathbf{r}_M \cdot \hat{\mathbf{y}}. \quad (19)$$

In this special case, the vertical motion of C is given by

$$\mathbf{r}_C(t) \cdot \hat{\mathbf{y}} = R\hat{\mathbf{y}} + \frac{1}{6}\mathbf{j}_C \cdot \hat{\mathbf{y}}t^3 + O(t^4). \quad (20)$$

The normal component of the jerk can be readily shown to be

$$\mathbf{j}_C \cdot \hat{\mathbf{y}} = \omega^3 r_M (\hat{\mathbf{x}} \cdot \hat{\mathbf{r}}_M). \quad (21)$$

We see that for a clockwise rotation (negative ω), the normal component of the center of mass velocity \mathbf{v}_M of body 2 is towards body 1. The normal component of the jerk \mathbf{j}_C is negative, indicating that the center of curvature C is moving in the $-\hat{\mathbf{y}}$ direction, and if $|\mathbf{v}_M \cdot \hat{\mathbf{x}}|$ is sufficiently small, its equidistant circular arc in the vicinity of point P necessarily penetrates body 1.

This is the essence of our paradox. In certain situations, the distance between the colliding bodies is proportional to t^3 . It follows that since the relative normal velocity is zero at the time of collision, there is no momentum transfer, since the bodies are rigid. The subsequent motion then leads to the interpenetration of rigid bodies – our paradox. We also provide, in Supplementary Data I, an example of a nonuniform disk, corresponding to the circle shown in with dashed lines in Fig. 1, colliding with a stationary line, which allows exact analytic description of the dynamics.

Below, we examine collisions in more detail.

4 Description of the Dynamics

4.1 General Description

Here we consider the motion of the points of contact on the colliding bodies, as well as of the points in the vicinity of the points of contact before and after collisions. We are interested in the

compatibility of particle motion with the conservation laws; we are particularly interested in the separation and possible interpenetration of the two colliding particles.

A convenient way to describe the closed surface of a body is by a dimensionless scalar function $G(t, \mathbf{r})$, representing level sets, such that, if $\mathbf{r}(t)$ is the position vector of a point on the surface of the body at time t , then

$$G(t, \mathbf{r}(t)) = 0. \quad (22)$$

The time t appears explicitly in the argument list to indicate that the position and the orientation of the body are, in general, changing in time. If

$$\hat{\mathbf{n}} = \frac{\nabla G}{|\nabla G|} \quad (23)$$

is the outward pointing unit normal, then $G(t, \mathbf{r}(t)) < 0$ indicates that the point designated by $\mathbf{r}(t)$ is inside the body, while $G(t, \mathbf{r}(t)) > 0$ indicates that it is outside. Since we are interested, in addition, in the distances between bodies, we introduce the signed distance

$$F(t, \mathbf{r}(t)) = G(t, \mathbf{r}(t))L, \quad (24)$$

where L is a suitably chosen length.

We now inquire whether an arbitrary point $\mathbf{r}_2(t)$ on the surface of body 2 at time t is inside, outside or on the surface, described by $F_1(t, \mathbf{r}(t)) = 0$, of body 1.

As we are probing collision kinematics, we are primarily interested in the relative locations of the points of contact, but we are also interested in the locations of material points on the surface in the neighborhood of the contact points just before, at, and just after the collision. Due to convexity, more distant points on the surface are also more distant from the tangent plane at the point of contact, hence we do not consider them here.

Except perhaps at the instant of collision, particles 1 and 2 are moving in space according to their force and torque-free equations of motion; that is, with constant linear and angular momenta, conserving kinetic energy. Their constants of motion, before and after the collision, are determined by initial conditions. The position vector of the point of contact P on body 1 is given by

$$\mathbf{r}_P = \mathbf{r}_{c1} + \mathbf{p}, \quad (25)$$

and similarly, the position vector of the point of contact Q on body 2 is given by

$$\mathbf{r}_Q = \mathbf{r}_{c2} + \mathbf{q}. \quad (26)$$

We introduce the body fixed small vector $\boldsymbol{\varepsilon}(t)$, from the point Q to a neighboring point on body 2. We constrain $\boldsymbol{\varepsilon}$ to be small by requiring that $\kappa\varepsilon \ll 1$, where κ is the maximum curvature of the normal sections of the surface at the point of contact. The position vector of this point is

$$\mathbf{r}_{Q+} = \mathbf{r}_{c2} + \mathbf{q} + \boldsymbol{\varepsilon}_Q. \quad (27)$$

We indicate the position of a point on the surface of body 2 in the vicinity of Q by the ‘+’ sign on the subscript of \mathbf{r}_{Q+} . It is useful to write $\boldsymbol{\varepsilon}_Q$ as

$$\boldsymbol{\varepsilon}_Q = -\varepsilon_{\parallel} \hat{\mathbf{n}}_2 + \boldsymbol{\varepsilon}_{\perp}, \quad (28)$$

where $\hat{\mathbf{n}}_2$ is the outward unit normal to body 2 at Q , $\varepsilon_{\parallel} > 0$ due to convexity, $\boldsymbol{\varepsilon}_{\perp}$ is perpendicular to $\hat{\mathbf{n}}_2$, and $\varepsilon_{\parallel} = O(\varepsilon_{\perp}^2)$ as shown in Supplementary Data II.

As the bodies move, points on the surfaces of the two bodies change their positions in space. The position $\mathbf{r}(t)$ of an arbitrary point on the surface of a body can be expanded in Taylor series about $t = 0$ to give

$$\begin{aligned} \mathbf{r}(t) &= \mathbf{r}(0) + \dot{\mathbf{r}}(0)t + \frac{1}{2}\ddot{\mathbf{r}}(0)t^2 + \frac{1}{6}\dddot{\mathbf{r}}(0)t^3 + O(t^4) \\ &= \mathbf{r}(0) + \mathbf{v}t + \frac{1}{2}\mathbf{a}t^2 + \frac{1}{6}\mathbf{j}t^3 + O(t^4), \end{aligned} \quad (29)$$

where \mathbf{v} , \mathbf{a} and \mathbf{j} are the velocity, acceleration and jerk. We note here that in collisions where the relative normal velocity is not zero, the coefficients of the powers of t may differ before and after the collision. If this is the case, we will indicate pre-collisions values of t by t_- , and post-collision values of t by t_+ . Explicit expressions for these in the free motion of rigid bodies are given in Supplementary Data III.

To determine if a point on the surface of particle 2 with position vector $\mathbf{r}_2(t)$ has penetrated body 1, we evaluate $F_1(t, \mathbf{r}_2(t))$.

It is useful to choose a specific form for $F_1(t, \mathbf{r}_Q(t))$. The surface of a smooth convex body in the vicinity of a point on the surface can be well described by the normal to the surface, and the two principal curvatures, and the associated principal directions in the tangent plane. We choose therefore $F_1(t, \mathbf{r})$ such that, in the vicinity of the point \mathbf{r}_P , one has

$$F_1(t, \mathbf{r}(t)) = (\mathbf{r} - \mathbf{r}_P) \cdot \hat{\mathbf{n}}_1 + \frac{1}{2}(\mathbf{r} - \mathbf{r}_P) \cdot \left(\frac{2\kappa_{1x}^2 \hat{\mathbf{x}}_1 \hat{\mathbf{x}}_1 + 2\kappa_{1y}^2 \hat{\mathbf{y}}_1 \hat{\mathbf{y}}_1}{|\mathbf{n}_1|} \right) \cdot (\mathbf{r} - \mathbf{r}_P) + O(|\mathbf{r} - \mathbf{r}_P|^3), \quad (30)$$

where $\mathbf{n}_1(t) = \nabla G_1$ is the outward normal, and we have chosen the length $L = 1/|\mathbf{n}_1|$. The symbols κ_{1x} and κ_{1y} , both strictly positive, are the principal curvatures, and $\hat{\mathbf{x}}_1(t)$ and $\hat{\mathbf{y}}_1(t)$ are

the corresponding eigenvectors. The Hessian of F_1 is

$$\mathbf{H}_1 = \frac{2\kappa_{1x}^2 \hat{\mathbf{x}}_1 \hat{\mathbf{x}}_1 + 2\kappa_{1y}^2 \hat{\mathbf{y}}_1 \hat{\mathbf{y}}_1}{|\mathbf{n}_1|}, \quad (31)$$

and so

$$F_1(t, \mathbf{r}(t)) = (\mathbf{r} - \mathbf{r}_P) \cdot \hat{\mathbf{n}}_1 + \frac{1}{2}(\mathbf{r} - \mathbf{r}_P) \cdot \mathbf{H}_1 \cdot (\mathbf{r} - \mathbf{r}_P) + O(|\mathbf{r} - \mathbf{r}_P|^3). \quad (32)$$

The function $F_1(t, \mathbf{r}(t))$ measures a signed distance between the point designated by $\mathbf{r}(t)$ and the surface of body 1.

To indicate points in the vicinity of the point Q at the time of collision, we write

$$\mathbf{r}_{Q+}(t) = \mathbf{r}_P(t) + \boldsymbol{\delta}_Q(t), \quad (33)$$

where

$$\boldsymbol{\delta}_Q(t) = \mathbf{r}_{Q+}(t) - \mathbf{r}_P(t) = \mathbf{r}_Q(t) - \mathbf{r}_P(t) + \boldsymbol{\varepsilon}_Q(t), \quad (34)$$

We then have

$$F_1(t, \mathbf{r}_{Q+}(t)) = \hat{\mathbf{n}}_1 \cdot \boldsymbol{\delta}_Q + \frac{1}{2} \boldsymbol{\delta}_Q \cdot \mathbf{H}_1 \cdot \boldsymbol{\delta}_Q + O(|\boldsymbol{\delta}_Q|^3). \quad (35)$$

To study the approach and separation of the colliding bodies, we evaluate $F_1(t, \mathbf{r}_{Q+}(t))$ as a function of time.

The collision occurs at time $t = 0$; hence we expand $F_1(t, \mathbf{r}_{Q+}(t))$ in Taylor series about $t = 0$:

$$F_1(t, \mathbf{r}_{Q+}(t)) = \left(\hat{\mathbf{n}}_1 \cdot \boldsymbol{\delta}_Q + \frac{1}{2} \boldsymbol{\delta}_Q \cdot \mathbf{H}_1 \cdot \boldsymbol{\delta}_Q \right) \Big|_{t=0} + \frac{\partial}{\partial t} \left(\hat{\mathbf{n}}_1 \cdot \boldsymbol{\delta}_Q + \frac{1}{2} \boldsymbol{\delta}_Q \cdot \mathbf{H}_1 \cdot \boldsymbol{\delta}_Q \right) \Big|_{t=0} t \quad (36)$$

$$+ \frac{1}{2} \frac{\partial^2}{\partial t^2} \left(\hat{\mathbf{n}}_1 \cdot \boldsymbol{\delta}_Q + \frac{1}{2} \boldsymbol{\delta}_Q \cdot \mathbf{H}_1 \cdot \boldsymbol{\delta}_Q \right) \Big|_{t=0} t^2 + O(\max(|\boldsymbol{\delta}_Q|^3, t^3)). \quad (37)$$

Substitution gives

$$\begin{aligned} F_1(t, \mathbf{r}_{Q+}(t)) &= (\hat{\mathbf{n}}_1 \cdot (\mathbf{v}_Q - \mathbf{v}_P))t \\ &+ \frac{1}{2}(2\dot{\hat{\mathbf{n}}}_1 \cdot (\mathbf{v}_Q - \mathbf{v}_P) + \hat{\mathbf{n}}_1 \cdot (\dot{\mathbf{v}}_Q - \dot{\mathbf{v}}_P) + (\mathbf{v}_Q - \mathbf{v}_P) \cdot \mathbf{H}_1 \cdot (\mathbf{v}_Q - \mathbf{v}_P))t^2 \\ &+ (\hat{\mathbf{n}}_1 \cdot \boldsymbol{\varepsilon}_Q + \frac{1}{2} \boldsymbol{\varepsilon}_Q \cdot \mathbf{H}_1 \cdot \boldsymbol{\varepsilon}_Q) \\ &+ (\dot{\hat{\mathbf{n}}}_1 \cdot \boldsymbol{\varepsilon}_Q + \hat{\mathbf{n}}_1 \cdot \dot{\boldsymbol{\varepsilon}}_Q + (\mathbf{v}_Q - \mathbf{v}_P) \cdot \mathbf{H}_1 \cdot \boldsymbol{\varepsilon}_Q + \dot{\boldsymbol{\varepsilon}}_Q \cdot \mathbf{H}_1 \cdot \boldsymbol{\varepsilon}_Q + \frac{1}{2} \boldsymbol{\varepsilon}_Q \cdot \dot{\mathbf{H}}_1 \cdot \boldsymbol{\varepsilon}_Q)t \\ &+ \frac{1}{2}(\ddot{\hat{\mathbf{n}}}_1 \cdot \boldsymbol{\varepsilon}_Q + 2\dot{\hat{\mathbf{n}}}_1 \cdot \dot{\boldsymbol{\varepsilon}}_Q + \hat{\mathbf{n}}_1 \cdot \ddot{\boldsymbol{\varepsilon}}_Q \\ &+ (\dot{\mathbf{v}}_Q - \dot{\mathbf{v}}_P) \cdot \mathbf{H}_1 \cdot \boldsymbol{\varepsilon}_Q + 2(\mathbf{v}_Q - \mathbf{v}_P) \cdot \dot{\mathbf{H}}_1 \cdot \boldsymbol{\varepsilon}_Q + 2(\mathbf{v}_Q - \mathbf{v}_P) \cdot \mathbf{H}_1 \cdot \dot{\boldsymbol{\varepsilon}}_Q \\ &+ \ddot{\boldsymbol{\varepsilon}}_Q \cdot \mathbf{H}_1 \cdot \boldsymbol{\varepsilon}_Q + 2\dot{\boldsymbol{\varepsilon}}_Q \cdot \dot{\mathbf{H}}_1 \cdot \boldsymbol{\varepsilon}_Q + \dot{\boldsymbol{\varepsilon}}_Q \cdot \mathbf{H}_1 \cdot \dot{\boldsymbol{\varepsilon}}_Q + \frac{1}{2} \boldsymbol{\varepsilon}_Q \cdot \dot{\mathbf{H}}_1 \cdot \boldsymbol{\varepsilon}_Q)t^2 \\ &+ O(\max(|\boldsymbol{\delta}_Q|^3, t^3)), \end{aligned} \quad (38)$$

and we note that all quantities on the right hand side of Eq. (38) are evaluated at $t = 0$. In the case of normal collisions, the velocities \mathbf{v}_P and \mathbf{v}_Q as well as the angular velocities $\boldsymbol{\omega}_1$ and $\boldsymbol{\omega}_2$ change instantaneously at the instant of collision. We therefore distinguish between pre-collision values at $t = 0^-$, and post-collision values at $t = 0^+$. In the case of tangential collisions, the velocities \mathbf{v}_P and \mathbf{v}_Q and the angular velocities $\boldsymbol{\omega}_1$ and $\boldsymbol{\omega}_2$ do not change, and the distinction is not required.

We next write the expression for $F_1(t, \mathbf{r}_{Q+}(t))$ in standard form,

$$F_1(t, \mathbf{r}_{Q+}(t)) = x_Q + v_Q t + \frac{1}{2} a_Q t^2 + \frac{1}{6} j_Q t^3 + O(t^4) + f(\boldsymbol{\varepsilon}_{\perp Q}, t), \quad (39)$$

where

$$f(\boldsymbol{\varepsilon}_{\perp Q}, t) = (x_{\varepsilon Q} \varepsilon_{\perp} + x_{2\varepsilon Q} \varepsilon_{\perp}^2) + v_{\varepsilon Q} \varepsilon_{\perp} t + O_{\varepsilon}(\max(\varepsilon_{\perp}^3, \varepsilon_{\perp}^2 t, \varepsilon_{\perp} t^2)), \quad (40)$$

refers to the distance of a neighbor point of point Q , defined by $\boldsymbol{\varepsilon}_{\perp}$ from body 1. Here we have introduced the symbol O_{ε} to denote ‘big O’ for neighbor points. The index number before the subscript ε denotes the power of ε_{\perp} appearing in the expression.

Explicitly, the constants in Eqs. (39) and (40) for the point of contact Q are

$$x_Q = 0, \quad (41)$$

$$v_Q = \hat{\mathbf{n}}_1 \cdot (\mathbf{v}_Q - \mathbf{v}_P), \quad (42)$$

$$a_Q = \hat{\mathbf{n}}_1 \cdot (\dot{\mathbf{v}}_Q - \dot{\mathbf{v}}_P) + 2(\boldsymbol{\omega}_1 \times \hat{\mathbf{n}}_1) \cdot (\mathbf{v}_Q - \mathbf{v}_P) + (\mathbf{v}_Q - \mathbf{v}_P) \cdot \mathbf{H}_1 \cdot (\mathbf{v}_Q - \mathbf{v}_P), \quad (43)$$

and the additional terms for the neighboring points are

$$x_{\varepsilon Q} = 0, \quad (44)$$

$$x_{2\varepsilon Q} = \frac{1}{2}(\hat{\boldsymbol{\varepsilon}}_{\perp} \cdot \mathbf{H}_2 \cdot \hat{\boldsymbol{\varepsilon}}_{\perp}) + \frac{1}{2}(\hat{\boldsymbol{\varepsilon}}_{\perp} \cdot \mathbf{H}_1 \cdot \hat{\boldsymbol{\varepsilon}}_{\perp}), \quad (45)$$

$$v_{\varepsilon Q} = \hat{\mathbf{n}}_1 \times (\boldsymbol{\omega}_2 - \boldsymbol{\omega}_1) \cdot \hat{\boldsymbol{\varepsilon}}_{\perp} + (\mathbf{v}_Q - \mathbf{v}_P) \cdot \mathbf{H}_1 \cdot \hat{\boldsymbol{\varepsilon}}_{\perp}, \quad (46)$$

The higher order terms have been omitted to save space, as they are not relevant to our development below. Higher order terms in Eq. (40) are given in Supplementary Data II for completeness.

4.2 Analysis of Collisions

We assume throughout that the bodies are well separated before the collision; that is, at $t < 0$, there are no shared points.

We now consider the values taken by $F_1(t, \mathbf{r}_{Q+}(t))$ during the collision. We begin with the general expression

$$F_1(t, \mathbf{r}_{Q+}(t)) = v_Q t + \frac{1}{2} a_Q t^2 + \frac{1}{6} j_Q t^3 + O(t^4) + f(\boldsymbol{\varepsilon}_{\perp Q}, t), \quad (47)$$

where

$$f(\boldsymbol{\varepsilon}_{\perp Q}, t) = (x_{\varepsilon Q} \varepsilon_{\perp} + x_{2\varepsilon Q} \varepsilon_{\perp}^2) + v_{\varepsilon Q} \varepsilon_{\perp} t + O_{\varepsilon}(\max(\varepsilon_{\perp}^3, \varepsilon_{\perp}^2 t, \varepsilon_{\perp} t^2)). \quad (48)$$

At the instant of collision, $f(\boldsymbol{\varepsilon}_{\perp Q}, 0) = x_{2\varepsilon Q} \varepsilon_{\perp}^2$. Neighboring points of Q on the surface of body 2, that are also on the surface of body 1, are those for which $f(\boldsymbol{\varepsilon}_{\perp Q}, t) = 0$, that is, the point Q , when $\varepsilon_{\perp} = 0$, and the points for which, at the lowest order in t ,

$$\varepsilon_{\perp} = -\frac{v_{\varepsilon Q}}{x_{2\varepsilon Q}} t + O(t^2). \quad (49)$$

Since

$$v_{\varepsilon Q} = [\hat{\mathbf{n}}_1 \times (\boldsymbol{\omega}_2 - \boldsymbol{\omega}_1) + 2(\mathbf{v}_Q - \mathbf{v}_P) \cdot \mathbf{H}_1] \cdot \hat{\boldsymbol{\varepsilon}}_{\perp} \quad (50)$$

and

$$x_{2\varepsilon Q} = \frac{1}{2} \hat{\boldsymbol{\varepsilon}}_{\perp} \cdot \mathbf{H}_2 \cdot \hat{\boldsymbol{\varepsilon}}_{\perp} + \frac{1}{2} \hat{\boldsymbol{\varepsilon}}_{\perp} \cdot \mathbf{H}_1 \cdot \hat{\boldsymbol{\varepsilon}}_{\perp} > 0, \quad (51)$$

Eq. (49) represents a closed curve on the surface of body 2, containing the point Q , and expanding in time. The shape of the curve resembles a figure of eight: one loop corresponding to $t < 0$, the other to $t > 0$. The curve may be regarded as representing the intersection of two bodies before, at and after collision, at small times t , *if there were no motion of the point Q* . Points on the surface of body 2 inside these loops are in the interior of body 1, points outside of the loops are outside. The points which penetrate the deepest into body 1, are those for which $f(\boldsymbol{\varepsilon}_{\perp Q}, t)$ is at a minimum with respect to ε_{\perp} , that is, such that

$$\frac{\partial f(\boldsymbol{\varepsilon}_{\perp Q}, t)}{\partial \varepsilon_{\perp}} = 0. \quad (52)$$

For these points, again at the lowest order in t ,

$$\varepsilon_{\perp} = -\frac{v_{\varepsilon Q}}{2x_{2\varepsilon Q}} t + O(t^2), \quad (53)$$

which represents a smaller figure of eight than that given by Eq. (49). For this extreme set of points, we obtain, on substitution,

$$f(\boldsymbol{\varepsilon}_{\perp}, t) = -\frac{v_{\varepsilon Q}^2}{4x_{2\varepsilon Q}} t^2 + \frac{1}{6} j_{Q+} t^3 + O_{\varepsilon}(t^4), \quad (54)$$

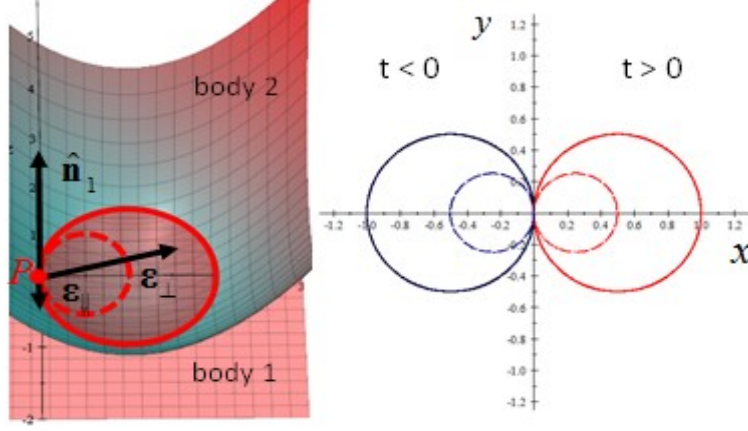


Figure 2: Figure of eight pattern illustrating penetration by neighboring points of Q that would occur if the point Q was not moving. The loops of the figure of eight need not be circles.

and

$$F_1(t, \mathbf{r}_{Q+}(t)) = v_Q t + \frac{1}{2} a_Q t^2 + \frac{1}{6} j_Q t^3 - \frac{v_{\varepsilon Q}^2}{4x_{2\varepsilon Q}} t^2 + \frac{1}{6} j_{Q+}^* t^3 + O(t^4) + O_\varepsilon(t^4), \quad (55)$$

and we see that the contribution of neighboring points is, to leading order, quadratic in time.

Now we write for potentially most deeply penetrating neighboring points on both bodies,

$$F_1(t, \mathbf{r}_{Q+}^*(t)) = v_Q t + \frac{1}{2} (a_Q - (\frac{v_{\varepsilon Q}^2}{2x_{2\varepsilon Q}})_{\max}) t^2 + \frac{1}{6} j_{Q+}^* t^3 + O_\varepsilon(t^4), \quad (56)$$

$$F_2(t, \mathbf{r}_{P+}^*(t)) = v_P t + \frac{1}{2} (a_P - (\frac{v_{\varepsilon P}^2}{2x_{2\varepsilon P}})_{\max}) t^2 + \frac{1}{6} j_{P+}^* t^3 + O_\varepsilon(t^4), \quad (57)$$

where max is over all possible directions ε_\perp , and we have established that

$$v_P = \hat{\mathbf{n}}_2 \cdot (\mathbf{v}_P - \mathbf{v}_Q) = v_Q, \quad (58)$$

$$a_P - (\frac{v_{\varepsilon P}^2}{2x_{2\varepsilon P}})_{\max} = a_Q - (\frac{v_{\varepsilon Q}^2}{2x_{2\varepsilon Q}})_{\max}. \quad (59)$$

The proof of the latter is given in Supplemental Data IV. These relations allow us to analyze the problem without bias on choice of body or of points. We next use these results in the arguments below.

4.2.1 Normal Collisions: $C_-(v < 0)$

In normal collisions, the normal speed of approach $v_{Qi} = \hat{\mathbf{n}}_1 \cdot (\mathbf{v}_{Qi} - \mathbf{v}_{Pi}) < 0$. It changes sign during the collision, so $v_f = -v_i$, and thus $v_Q t > 0$ both before and after the collision. It follows that for point Q

$$F_1(t, \mathbf{r}_Q(t)) = v_Q t + \frac{1}{2} a_Q t^2 + O(t^3) > 0, \quad (60)$$

and hence, in a normal collision, the contact point Q approaches body 1, comes into contact with the point P , then recedes. Convexity prevents the neighboring points from contact with body 1, as shown by

$$F_1(t, \mathbf{r}_{Q+}^*(t)) = v_Q t + \frac{1}{2}(a_Q - (\frac{v_{\varepsilon Q}^2}{2x_{2\varepsilon Q}})_{\max})t^2 + \frac{1}{6}j_{Q+}^* t^3 + O_{\varepsilon}(t^4). \quad (61)$$

Here j_{Q+}^* designates the jerk for the most deeply penetrating point in the set of Q and its neighbors. The same argument holds for point P and its neighbors on body 1. This scenario can be realized in the 2D paradigm if $\mathbf{v}_M \cdot \hat{\mathbf{y}} < \boldsymbol{\omega} \times \mathbf{r}_M \cdot \hat{\mathbf{y}}$.

4.2.2 Tangential Collisions: $C_0(v = 0)$

In tangential collisions, the normal speed of approach $v_Q = \hat{\mathbf{n}}_1 \cdot (\mathbf{v}_Q - \mathbf{v}_P) = 0$. This is an occasional event: the normal component of the velocity difference of the contact points must vanish at the instant of collision. As shown by Eq. (7), there is no momentum transfer, hence there are no changes in either the linear or the angular velocities. The post collisional behavior is indicated by the next terms in the expansion, as analyzed below.

Case C_{0+} If $a > (\frac{v_{\varepsilon}^2}{2x_{2\varepsilon}})_{\max}$, then for potentially most deeply penetrating neighboring points

$$F_1(t, \mathbf{r}_{Q+}^*(t)) = \frac{1}{2}(a_Q - (\frac{v_{\varepsilon Q}^2}{2x_{2\varepsilon Q}})_{\max})t^2 + \frac{1}{6}j_{Q+}^* t^3 + O_{\varepsilon}(t^4) > 0. \quad (62)$$

The coefficient of the quadratic term is positive, and for small t , the point Q and its neighbors do not penetrate body 1. The same argument holds for point P and its neighbors on body 1. Thus there is no interpenetration of two bodies either before or after the collision. This case corresponds to the 2D paradigm if $\mathbf{r}_C \cdot \hat{\mathbf{y}} < \mathbf{r}_M \cdot \hat{\mathbf{y}}$.

Case C_{0-} If $a < (\frac{v_{\varepsilon}^2}{2x_{2\varepsilon}})_{\max}$, then for potentially most deeply penetrating neighboring points

$$F_1(t, \mathbf{r}_{Q+}^*(t)) = \frac{1}{2}(a_Q - (\frac{v_{\varepsilon Q}^2}{2x_{2\varepsilon Q}})_{\max})t^2 + \frac{1}{6}j_{Q+}^* t^3 + O_{\varepsilon}(t^4) < 0. \quad (63)$$

For small t , there is penetration of body 1 by Q or its neighbors before and after the collision. This implies that the bodies were not well separated before the collision, hence the initial conditions leading to this collision cannot be realized. This case corresponds to the 2D paradigm if $\mathbf{r}_C \cdot \hat{\mathbf{y}} > \mathbf{r}_M \cdot \hat{\mathbf{y}}$.

Case C₀₀ A paradox! If $a = (\frac{v_\varepsilon^2}{2x_{2\varepsilon}})_{\max}$, for the potentially most deeply penetrating neighboring points we have

$$F_1(t, \mathbf{r}_{Q+}^*(t)) = \frac{1}{6}j_{Q+}^*t^3 + O_\varepsilon(t^4), \quad (64)$$

$$F_2(t, \mathbf{r}_{P+}^*(t)) = \frac{1}{6}j_{P+}^*t^3 + O_\varepsilon(t^4). \quad (65)$$

If the cubic terms don't vanish, then *we face a paradox*: the two bodies, initially well separated, come to rest at the instant of collision $t = 0$, and begin to move and interpenetrate after the collision. This is our key result: the dynamics of freely moving convex bodies can bring them into contact so that the separation between them is cubic in time. At the instant of collision the velocity of approach is zero, hence for rigid bodies there can be no momentum exchange. The motion continues, and since the relative acceleration is also zero, the continuing motion leads to interpenetration. This case corresponds to the 2D paradigm if $\mathbf{r}_C \cdot \hat{\mathbf{y}} = \mathbf{r}_M \cdot \hat{\mathbf{y}}$. Specific examples are provided in Supplementary Data I.

Below, we discuss the three different types of paradoxes that can arise for the two bodies, distinguished by the contact point behavior.

Type I: $a_P > 0, a_Q > 0$ For the distance of P and Q from the opposite body, we have

$$F_1(t, \mathbf{r}_Q(t)) = \frac{1}{2}a_Qt^2 + \frac{1}{6}j_Qt^3 + O(t^4), \quad (66)$$

$$F_2(t, \mathbf{r}_P(t)) = \frac{1}{2}a_Pt^2 + \frac{1}{6}j_Pt^3 + O(t^4). \quad (67)$$

Both contact points P and Q approach the other body, and comes into contact, and recede from the other body. In this case, the immediate interpenetration of two bodies is only through the immediate neighboring points of P and Q . This can be realized in the 2D paradigm if $\mathbf{v}_M \cdot \hat{\mathbf{x}} \neq 0$.

Type II: $a_P = 0, a_Q > 0$ In this case, for the distance of P and Q from the opposite body, we have

$$F_1(t, \mathbf{r}_Q(t)) = \frac{1}{2}a_Qt^2 + \frac{1}{6}j_Qt^3 + O(t^4), \quad (68)$$

$$F_2(t, \mathbf{r}_P(t)) = \frac{1}{6}j_Pt^3 + O(t^4). \quad (69)$$

The contact point P on body 1 and its immediate neighbors enter the body 2 following the collision. The contact point Q on body 2 approaches, come into contact, and recedes from body 1. The penetration into body 1 is through immediate neighboring points of Q . This can be realized in the 2D paradigm if $\mathbf{v}_M \cdot \hat{\mathbf{x}} = 0$.

Type III: $a_P = 0, a_Q = 0$ In this case, for the distance of P and Q from the opposite body, we have

$$F_1(t, \mathbf{r}_Q(t)) = \frac{1}{6}j_Q t^3 + O(t^4), \quad (70)$$

$$F_2(t, \mathbf{r}_P(t)) = \frac{1}{6}j_P t^3 + O(t^4). \quad (71)$$

The contact points P and Q together with their immediate neighbors both enter the opposite body following the collision. This scenario cannot occur in the 2D paradigm when one body is at rest.

We illustrate this example by the following special case. We consider the case with the additional constraint that the relative tangential velocity is also zero; that is, $\mathbf{v}_Q - \mathbf{v}_P = \mathbf{0}$. This only makes the conditions $v_Q = a_Q = v_{\varepsilon Q} = 0$ more easily realizable in simulations. As before, for small t , $F_1(t, \mathbf{r}_{Q+}(t)) > 0$ before the collision and $F_1(t, \mathbf{r}_{Q+}(t)) < 0$ after the collision, indicating that initial conditions for such a collision may be realized. With the additional constraint $\mathbf{v}_Q - \mathbf{v}_P = \mathbf{0}$, however, the condition $a = 0$ requires that $\hat{\mathbf{n}}_1 \cdot (\dot{\mathbf{v}}_Q - \dot{\mathbf{v}}_P) < 0$. This cannot be achieved for convex bodies in 2D. Interestingly, for freely moving homogeneous ellipsoids, $\mathbf{a} \cdot \hat{\mathbf{n}} \leq 0$. The proof of this is provided in Supplementary Data IV. Consequently, the condition $\hat{\mathbf{n}}_1 \cdot (\dot{\mathbf{v}}_Q - \dot{\mathbf{v}}_P) < 0$ cannot be achieved with ellipsoids. To demonstrate such a collision, showing the penetration of the point Q into body 1, we have constructed an example of a collision between an ellipsoid and a super-ellipsoid, where the ellipsoid penetrates the super-ellipsoid after the collision. The details are given in Supplementary Data I and the corresponding motion is rendered in the accompanying movie.

The family of collisions corresponding to the various constraints are shown in the flowchart of Fig. 3.

5 Conclusion

We have considered above the collisions of smooth, strictly-convex rigid bodies in 2D and 3D.

There are two types of collisions: the usual normal collisions, and the less usual tangential collisions.

In the case of normal collisions, when the velocity of approach of two contact points has a non-vanishing component along the normal to the surface at the point of contact, then there will be momentum transfer between the two bodies, and the contact points separate immediately after the collision. Furthermore, due to the strict convexity assumption, domains of points surrounding the contact points on two surfaces also separate immediately after the collision. More distant

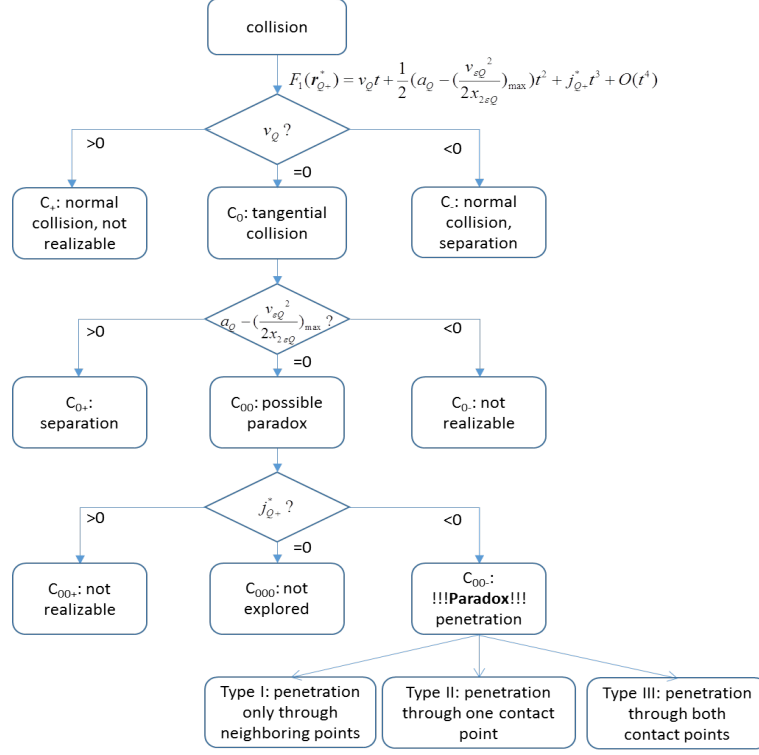


Figure 3: A flowchart illustrating the family of collisions and indicating where the paradox occurs.

points cannot penetrate the other body in zero time, since velocities are finite. Hence there is no interpenetration of bodies immediately after collision in the case of normal collisions.

In the case of tangential collisions, when the contact points approach each other with a non-zero finite velocity only along the tangent to the surfaces at the point of contact, then there is no momentum transfer, and the two bodies pass each other without any interaction. Our analysis shows that under certain circumstances, interpenetration occurs immediately after the collision; this is our paradox. Simple illustrative examples are given in 2D where one convex body collides with another at rest. We distinguish three different types of interpenetration, characterized by the behavior of the contact points. We have shown that the conservation of momentum and energy lead to the interpenetration of non-spherical convex rigid bodies, which violates their impenetrability. We conclude therefore that the dynamics of strictly-convex rigid bodies is not consistent with the conservation laws of classical mechanics. Specifically, the inconsistency means that the conservation laws (conservation of linear and angular momentum, and of energy) and rigidity (with necessarily instantaneous collisions with infinite force and the conservation of kinetic energy) cannot hold simultaneously in all collisions. We have enforced the conservation laws in our approach,

and observed that on some occasions rigidity is violated. Alternatively, we could have enforced momentum conservation and rigidity, and could have shown that, on some occasions, energy conservation is violated, thus making our paradox for smooth rigid bodies akin to those already known for rough rigid bodies.

The physical origins of the inconsistency are associated with the unrealistic hard interaction, which prevents the (temporary) storage of energy in the interaction potential. In the cases considered here, where jerk dominates, the contact points behave as though they experience time dependent force which is linear in time, giving rise to zero speed and acceleration but nonzero jerk at $t = 0$, followed by motion with acceleration in the same direction. In such a situation, a soft body would respond by gradually deforming after the collision, and temporarily storing/dissipating energy in the deformation as a function of time. This behavior is disallowed for rigid bodies, where kinetic energy alone must be conserved.

For non-convex rigid bodies, the collision dynamics would be much more complicated and we have not considered it here.

In conclusion, we have presented a new paradox: as shown by our theory and illustrated by examples, the dynamics of smooth convex rigid bodies is not consistent with the conservation laws of classical mechanics.

5.0.1 Data accessibility.

All the data used in this paper are already present in the ancillary Supplementary Data document.

5.0.2 Authors' contributions.

The work was undertaken by X.Z. and P. P-M., following the suggestion of M.W. The group of X.Z., P.P-M. and M.W. was subsequently joined by E.G.V. who enlarged the scope of the project. The paper was jointly written by all authors.

5.0.3 Competing interests.

The authors have no competing interests.

5.0.4 Funding.

P.P-M. and X.Z. were funded for part of this work by the NSF under DMS-1212046.

5.0.5 Acknowledgements.

P.P.-M. and X.Z. acknowledge support from NSF under DMS-1212046. Most of this work was done while E.G.V. was visiting the Oxford Centre for Nonlinear PDE at the University of Oxford, whose kind hospitality he gratefully acknowledges. We are grateful to the referees for their comments and suggestions. We are particularly grateful to Referee 2, whose insightful comments and suggestions resulted in new results and significant improvements to the work presented here.

References

- [1] S. Lem, *The Cyberiad: The Dragons of Probability*, Harvest Books, (2002).
- [2] B. Brogliato, *Nonsmooth Mechanics-Models, Dynamics and Control*, 3rd ed., Springer, London, 2016.
- [3] L. Saint-Raymond and M. Wilkinson, ‘On collision invariants for linear scattering’, arXiv:1507.07601v1, (2015).
- [4] A. Chatterjee, ‘Two interpretations of rigidity in rigid-body collisions’, *J. Appl. Mech.* **65**, 894 (1998).
- [5] A. Chatterjee, ‘A new algebraic rigid-body collision law based on impulse space considerations’. *J. Appl. Mech.* **65**, 939 (1998).
- [6] P. Painlevé, ‘Sur les lois du frottement de glissement’, *C. R. Acad. Sci. Paris*, **121**, 112 (1985). (Articles under the same title also appeared in *C. R. Acad. Sci. Paris* **141**, 401 and 546).
- [7] D. E. Stewart, ‘Rigid-body dynamics with friction and impact’, *SIAM Review*, **42**, 3 (2000).
- [8] O. C. Dyre, ‘Simple liquids quasiuniversality and the hard-sphere paradigm’, *J. Phys.: Condens. Matter*, **12**, 32301, (2016).
- [9] H. Goldstein, *Classical Mechanics*, 2nd ed., Addison-Wesley, (1980).
- [10] F. S. Crawford, ‘A theorem on elastic collisions between ideal rigid bodies’, *Am J Phys.* **57**, 121, (1989).
- [11] Ch. Glocker, ‘On frictionless impact models in rigid-body systems’, *Phil. Trans. R. Soc. Lond. A*, **259**, 2385 (2001).

- [12] W. J. Stronge, ‘Rigid body collisions with friction’, Proc. R. Soc. Lond. A, **431**, 169 (1990).
- [13] T. R. Kane, ‘A dynamics puzzle’, Stanford Mechanics Alumni Club Newsletter, **53** (1984).
- [14] J. B. Keller, ‘Impact with friction’, J. Appl. Mech., **53**, 1 (1986).
- [15] R. M. Brach, ‘Rigid body collisions’, J. Appl. Mech. **56**, 1233 (1989).
- [16] C. W. Kilmister, J. E. Reeve, Rational Mechanics. London:Longman (1966).

6 Supplementary Data

6.1 Part I: Examples

6.1.1 2D Example: Collision of a nonuniform circle and a rigid wall

Here we provide a 2D example, where the details of the collision are given exactly in analytic form.

Consider a disk of radius R_0 with a non-homogeneous mass distribution, such that the location of the center of mass M of the disk differs from its geometric center C . (This is equivalent to replacing body 1, the homogeneous ellipse, in Fig. 1 in the 2D Paradigm section, by an inhomogeneous circular disk, and replacing the boundary of body 2 by a straight line.) The moving disk collides with a

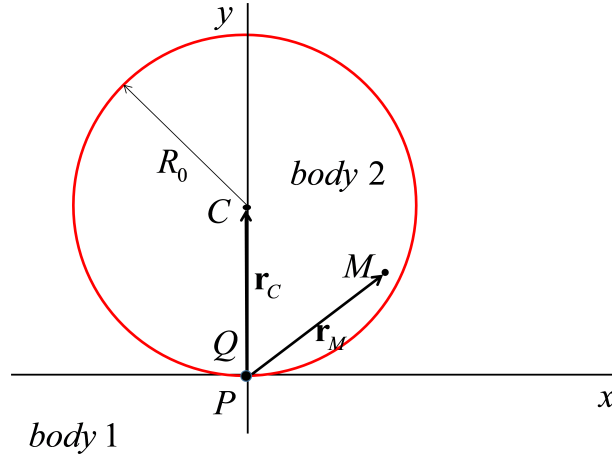


Figure 4: A non-homogeneous disk (body 2) of radius R_0 colliding with a wall (body 1) in an inertial frame. M is the center of mass of the disk, which differs from its geometric center C . Q is the contact point on the disk. P is the contact point on the line, which we designate as the origin. The contact normal of body 1 is along the $\hat{\mathbf{y}}$ direction. The disk is moving with linear velocity \mathbf{v}_M , and rotate with angular velocity ω .

line at rest along the x -axis in an inertial frame. The points of contact at the instant of collision are P in body 1, and Q in body 2. We denote by θ the angle that the vector \mathbf{r}_C makes with $\hat{\mathbf{y}}$, and θ_M is the angle that vector \mathbf{r}_M makes with $\hat{\mathbf{y}}$. That is,

$$r_{Cx} = -R_0 \sin \theta, \quad (72)$$

$$r_{Cy} = R_0 \cos \theta, \quad (73)$$

and similarly,

$$r_{Mx} = -r_M \sin \theta_M, \quad (74)$$

$$r_{My} = r_M \cos \theta_M. \quad (75)$$

We consider the case when the collision is tangential, that is, the normal velocity of the point on the disk in contact with the line is zero. Hence there is no momentum transfer, and the disk will move with constant linear and angular velocity. We are particularly interested in the motion of points Q and C . Rigid body kinematics prescribes that

$$\mathbf{v}_Q = \mathbf{v}_M - \boldsymbol{\omega} \times \mathbf{r}_M, \quad (76)$$

where \mathbf{v}_Q and \mathbf{v}_M the velocities of the points Q and M .

Then

$$v_{Qx} = v_{Mx} + \omega r_M \cos \theta_M, \quad (77)$$

$$v_{Qy} = v_{My} + \omega r_M \sin \theta_M, \quad (78)$$

and this can be integrated at once to give

$$Q_x(t) = v_{Mx}t + r_M(\sin(\theta_M(0) + \omega t) - \sin(\theta_M(0))), \quad (79)$$

$$Q_y(t) = v_{My}t - r_M(\cos(\theta_M(0) + \omega t) - \cos(\theta_M(0))), \quad (80)$$

where we have assumed that Q is at the origin at the instant of collision $t = 0$. The tangential collision at $t = 0$ implies $v_{My} = -\omega r_M \sin \theta_M(0)$.

Similarly, for C ,

$$\mathbf{v}_C = \mathbf{v}_M + \boldsymbol{\omega} \times (\mathbf{r}_C - \mathbf{r}_M), \quad (81)$$

we have

$$v_{Cx} = v_{Mx} - \omega(R_0 \cos \theta - r_M \cos \theta_M), \quad (82)$$

$$v_{Cy} = v_{My} - \omega(R_0 \sin \theta - r_M \sin \theta_M). \quad (83)$$

Integration gives (on taking $\theta(0) = 0$)

$$C_x = v_{Mx}t - R_0 \sin \omega t + r_M(\sin(\theta_M(0) + \omega t) - \sin(\omega_M(0))), \quad (84)$$

$$C_y = R_0 - \omega r_M \sin \theta_M(0)t + R_0(\cos \omega t - 1) - r_M(\cos(\theta_M(0) + \omega t) - \cos(\theta_M(0))). \quad (85)$$

The Eqs. (84) and (85) completely and exactly describe the motion of the disk.

We now examine the motion of the bottom of the disk relative to the line. Here only the y -component matters, and we have, for small t ,

$$C_y - R_0 = \frac{1}{2}(r_M \cos \theta_M(0) - R_0)\omega^2 t^2 - \frac{1}{6}r_M \sin \theta_M(0)\omega^3 t^3 + O(t^4). \quad (86)$$

If $r_M \cos \theta_M(0) > R_0$, then $C_y - R_0 > 0$ for any small $t \neq 0$, which indicates that there is no interpenetration of the disk with the wall either before or after the collision, corresponding to the case C_{0+} .

If $r_M \cos \theta_M(0) < R_0$, then $C_y - R_0 < 0$ for any small $t \neq 0$, indicates that there is interpenetration of the disk by the wall both before and after the collision, corresponding to the case C_{0-} .

If $r_M \cos \theta_M(0) = R_0$, and $\omega < 0$, then this leads to our paradox C_{00+} .

For this 2D example, we further construct the Type I and Type II paradoxes. We look at the motion of Q . Here only the y - component matters, and we have, for small t ,

$$Q_y(t) = \frac{1}{2}R_0\omega^2 t^2 + \frac{1}{6}d\omega^3 t^3 + O(t^4), \quad (87)$$

where

$$d = \sqrt{r_M^2 - R_0^2}. \quad (88)$$

Since $Q_y(t) > 0$ for small t , Q stays above the line; it does not penetrate body 1.

We now look at the position of P relative to the disk. Since

$$C_x = v_{Mx}t + \frac{1}{2}d\omega^2 t^2 + O(t^4), \quad (89)$$

$$C_y - R_0 = -\frac{1}{6}d\omega^3 t^3 + O(t^4), \quad (90)$$

the intersection of the disk with the x axis, where $y = 0$, occurs at the points

$$x = v_{Mx}t + \frac{1}{2}d\omega^2 t^2 \pm \frac{1}{\sqrt{3}}\sqrt{R_0 d \omega^3} t^{3/2} + O(t^{5/2}). \quad (91)$$

We distinguish two cases.

If $v_{Mx} \neq 0$, at short times, the term linear in t dominates, and both intersection points are either positive or negative; they are both on one side of P . Thus P doesn't penetrate the disk, body 2, immediately after the collision. In this case, the interpenetration is through neighboring points of P and neighboring points of Q only, this corresponds to our Type I paradox.

If $v_{Mx} = 0$, the term of order $t^{3/2}$ dominates, and one intersection point is positive, and the other is negative; they bracket P . Thus both the point P and its immediate neighbors enter the

disk, but only the points neighboring Q in the disk penetrate body 1. This corresponds to our Type II paradox.

We remark that we cannot construct the Type III paradox in this example, where, in 2D, one of the bodies is stationary.

A brief video is provided in the following link:

<http://www.math.kent.edu/~zheng/papers/animationDisk.gif>

6.1.2 2D Example: collision of Two Ellipses

We note that here, and in subsequent examples, we give initial conditions with machine precision to enable interested readers to duplicate our simulation, and verify our results.

Both ellipses have semi-axes lengths $a = 2, b = 1$.

The center of mass of ellipse 1 is at $(0, 0)$.

The long axis of ellipse 1 is along $(1, 0)$.

The contact point P at ellipse 1 is $(-1.5118578920369088, -0.6546536707079771)$.

The contact normal is $\hat{\mathbf{n}}_1 = (-1/2, -\sqrt{3}/2)$.

The velocity of the center of mass of ellipse 1 is $(0, 0)$.

The angular velocity of ellipse 1 is $(0, 0, -1)$.

The center of mass of ellipse 2 is at $(-1.4671103616817882, -1.9459065947411789)$.

The long axis of ellipse 2 points along $(1/\sqrt{2}, -1/\sqrt{2})$.

The contact point Q at ellipse 2 is $(-0.04474753035512054, 1.2912529240332018)$.

The velocity of the center of mass of ellipse 2 is $(-0.2139701987389151, 0.9581598646385255)$.

The angular velocity of ellipse 2 is $(0, 0, -0.3787007446061675)$. This is Type II paradox, when one contact point flies away, and the other contact point enters the opposite body. A brief animation is provided in the following link:

<http://www.math.kent.edu/~zheng/papers/animation2D.gif>

6.1.3 3D Example: Collision of a Superellipsoid and an Ellipsoid

The first body is a superellipsoid described by the equation

$$\frac{x^4}{a^4} + \frac{y^4}{b^4} + \frac{z^4}{c^4} = 1,$$

with $a = 1, b = 2, c = 3$.

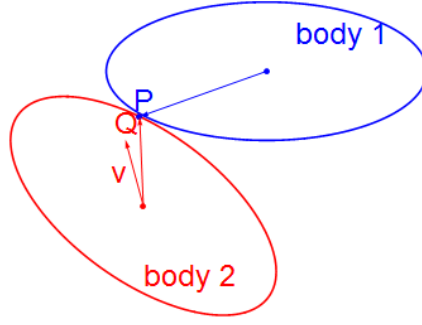


Figure 5: The configuration of two ellipses at the time of collision. The vector \mathbf{v} emitting from the center of body 2 indicates the linear velocity of body 2. The linear velocity of the first body is zero. Both ellipses rotates clockwise. The angular velocity of body 1 is -1 , and angular velocity of body 2 is -0.378 . They interpenetrate each other immediately after the collision.

The center of mass of superellipsoid 1 is at $(0, 0, 0)$.

The contact point P at superellipsoid 1 is

$(0.47618533191703555, 1.9605250610979892, 1.1955976303024505)$.

The contact normal is

$\hat{\mathbf{n}}_1 = (0.22325108832916085, 0.9737842723056427, 0.04362502229243368)$.

The velocity of center of mass of superellipsoid 1 is $(0, 0, 0)$.

The angular velocity of superellipsoid 1 is

$(1.1740747914710616, 5.121119789388775, 1.2294234681418093)$.

Ellipsoid 2 with semiaxes length $a' = 2, b' = c' = 1$, and pointing along $(0, 0, 1)$,

$(0.6239979329820173, 0.781425991143224, 0)$,

$(-0.781425991143224, 0.6239979329820173, 0)$, respectively.

The center of mass of ellipsoid 2 is at

(0.6988018183920255, 2.931541305218898, 1.3696016946556036).

The contact point Q at ellipsoid 2 is

(0.47618533191703555, 1.9605250610979892, 1.1955976303024505).

The velocity of center of mass of ellipsoid 2 is

(2.7414669205732727, -0.5956711297619547, -0.1367990744145808).

The angular velocity of ellipsoid 2 is $(0, 0, 1)$.

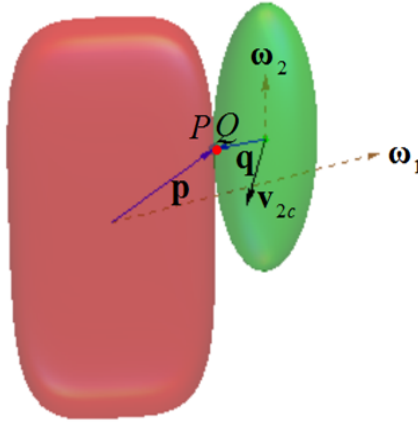


Figure 6: The illustration shows the configuration of the superellipsoid and ellipsoid at the time of collision. The body-fixed vectors \mathbf{p} and \mathbf{q} meet at the contact point. The vectors with dashed lines from the centers of the two bodies represent angular velocities, and the third solid arrow from center of the ellipsoid represents the velocity of its center of mass. Immediately after the collision, the point P and its neighbors penetrate body 2, the ellipsoid, and the point Q and its neighbors penetrate body 1, the superellipsoid. A link to an animation of the collision is provided below.

This is a type III paradox, where both contact points penetrate the opposite body. We also note that if we let the ellipsoid spins with respect to its long axis with any other angular velocity, then this will correspond to type II paradox, the contact point on the ellipsoid won't penetrate the superellipsoid. A brief animation is provided in the following link:

<http://www.math.kent.edu/~zheng/papers/animation3D.gif>

An animation of the collision between the superellipsoid and the ellipsoid is shown on the left; the animation on the right is a blow-up of the region near the contact point P and Q . The

penetration of the superellipsoid into the ellipsoid can be clearly seen in the blown-up region on the right.

6.2 Part II: Essential Information

6.2.1 Epsilon

Since ε_Q denotes a neighboring point of Q it must lie on the surface of body 2. It must therefore satisfy

$$F_2(\varepsilon_Q) = \hat{\mathbf{n}}_2 \cdot \varepsilon_Q + \frac{1}{2} \varepsilon_Q \cdot \mathbf{H}_2 \cdot \varepsilon_Q + O(|\varepsilon_Q|^3) = 0. \quad (92)$$

Writing

$$\varepsilon_Q = -\varepsilon_{\parallel} \hat{\mathbf{n}}_2 + \varepsilon_{\perp}, \quad (93)$$

we have

$$-\varepsilon_{\parallel} + \frac{1}{2} \varepsilon_{\perp} \cdot \mathbf{H}_2 \cdot \varepsilon_{\perp} + O(|\varepsilon_Q|^3) = 0, \quad (94)$$

or

$$\varepsilon_{\parallel} = \varepsilon_{\perp}^2 \frac{1}{2} \hat{\varepsilon}_{\perp} \cdot \mathbf{H}_2 \cdot \hat{\varepsilon}_{\perp} + O(|\varepsilon_Q|^3). \quad (95)$$

6.2.2 Summary of standard form

The standard form of $F_1(t, \mathbf{r}_{Q+}(t))$ for small t is

$$\begin{aligned} F_1(t, \mathbf{r}_{Q+}(t)) &= x_Q + v_Q t + \frac{1}{2} a_Q t^2 + \frac{1}{6} j_Q t^3 + O(t^4) \\ &\quad + (x_{\varepsilon_Q} \varepsilon_{\perp} + x_{2\varepsilon_Q} \varepsilon_{\perp}^2) + (v_{\varepsilon_Q} \varepsilon_{\perp} + v_{2\varepsilon_Q} \varepsilon_{\perp}^2 + v_{3\varepsilon_Q} \varepsilon_{\perp}^3) t \\ &\quad + \frac{1}{2} (a_{\varepsilon_Q} \varepsilon_{\perp} + a_{2\varepsilon_Q} \varepsilon_{\perp}^2) t^2 + \frac{1}{6} j_{\varepsilon_Q} t^3 + O_{\varepsilon}(t^4), \end{aligned} \quad (96)$$

where

$$x_Q = 0, \quad (97)$$

$$v_Q = \hat{\mathbf{n}}_1 \cdot (\mathbf{v}_Q - \mathbf{v}_P), \quad (98)$$

$$a_Q = 2(\boldsymbol{\omega}_1 \times \hat{\mathbf{n}}_1) \cdot (\mathbf{v}_Q - \mathbf{v}_P) + \hat{\mathbf{n}}_1 \cdot (\dot{\mathbf{v}}_Q - \dot{\mathbf{v}}_P) + (\mathbf{v}_Q - \mathbf{v}_P) \cdot \mathbf{H}_1 \cdot (\mathbf{v}_Q - \mathbf{v}_P), \quad (99)$$

for the point of contact Q , and

$$x_{2\varepsilon} = \frac{1}{2} (\hat{\varepsilon}_{\perp} \cdot \mathbf{H}_1 \cdot \hat{\varepsilon}_{\perp}) + \frac{1}{2} (\hat{\varepsilon}_{\perp} \cdot \mathbf{H}_2 \cdot \hat{\varepsilon}_{\perp}), \quad (100)$$

and

$$v_\varepsilon = \hat{\mathbf{n}}_1 \times (\boldsymbol{\omega}_2 - \boldsymbol{\omega}_1) \cdot \hat{\boldsymbol{\varepsilon}}_\perp + (\mathbf{v}_Q - \mathbf{v}_P) \cdot \mathbf{H}_1 \cdot \hat{\boldsymbol{\varepsilon}}_\perp, \quad (101)$$

$$v_{2\varepsilon} = (\boldsymbol{\omega}_2 \times \hat{\boldsymbol{\varepsilon}}_\perp) \cdot \mathbf{H}_1 \cdot \hat{\boldsymbol{\varepsilon}}_\perp + \frac{1}{2} \hat{\boldsymbol{\varepsilon}}_\perp \cdot \dot{\mathbf{H}}_1 \cdot \hat{\boldsymbol{\varepsilon}}_\perp, \quad (102)$$

$$v_{3\varepsilon} = h(\hat{\boldsymbol{\varepsilon}}_\perp)(\boldsymbol{\omega}_2 \times \dot{\hat{\mathbf{n}}}_1) \cdot \mathbf{H}_1 \cdot \hat{\boldsymbol{\varepsilon}}_\perp + h(\hat{\boldsymbol{\varepsilon}}_\perp) \hat{\mathbf{n}}_1 \cdot \dot{\mathbf{H}}_1 \cdot \hat{\boldsymbol{\varepsilon}}_\perp, \quad (103)$$

$$v_{4\varepsilon} = \frac{1}{2} h^2(\hat{\boldsymbol{\varepsilon}}_\perp) \hat{\mathbf{n}}_1 \cdot \ddot{\mathbf{H}}_1 \cdot \hat{\mathbf{n}}_1, \quad (104)$$

and

$$\begin{aligned} a_\varepsilon = & (\dot{\boldsymbol{\omega}}_1 \times \hat{\mathbf{n}}_1) \cdot \hat{\boldsymbol{\varepsilon}}_\perp + (\boldsymbol{\omega}_1 \cdot \hat{\mathbf{n}}_1)(\boldsymbol{\omega}_1 \cdot \hat{\boldsymbol{\varepsilon}}_\perp) + 2(\hat{\boldsymbol{\varepsilon}}_\perp \cdot \hat{\mathbf{n}}_1)(\boldsymbol{\omega}_1 \cdot \boldsymbol{\omega}_2) \\ & - 2(\hat{\boldsymbol{\varepsilon}}_\perp \cdot \boldsymbol{\omega}_1)(\boldsymbol{\omega}_2 \cdot \hat{\mathbf{n}}_1) + \hat{\boldsymbol{\varepsilon}}_\perp \cdot (\hat{\mathbf{n}}_1 \times \dot{\boldsymbol{\omega}}_2) + (\hat{\mathbf{n}}_1 \cdot \boldsymbol{\omega}_2)(\boldsymbol{\omega}_2 \cdot \hat{\boldsymbol{\varepsilon}}_\perp) \\ & + (\dot{\mathbf{v}}_Q - \dot{\mathbf{v}}_P) \cdot \mathbf{H}_1 \cdot \hat{\boldsymbol{\varepsilon}}_\perp + 2(\mathbf{v}_Q - \mathbf{v}_P) \cdot \dot{\mathbf{H}}_1 \cdot \hat{\boldsymbol{\varepsilon}}_\perp + 2(\mathbf{v}_Q - \mathbf{v}_P) \cdot \mathbf{H}_1 \cdot (\boldsymbol{\omega}_2 \times \hat{\boldsymbol{\varepsilon}}_\perp), \end{aligned} \quad (105)$$

$$\begin{aligned} a_{2\varepsilon} = & -h(\hat{\boldsymbol{\varepsilon}}_\perp) \boldsymbol{\omega}_1 \cdot (\mathbb{I} - \hat{\mathbf{n}}_1 \hat{\mathbf{n}}_1) \cdot \boldsymbol{\omega}_1 + 2h(\hat{\boldsymbol{\varepsilon}}_\perp) \boldsymbol{\omega}_1 \cdot (\mathbb{I} - \hat{\mathbf{n}}_1 \hat{\mathbf{n}}_1) \cdot \boldsymbol{\omega}_2 \\ & - h(\hat{\boldsymbol{\varepsilon}}_\perp) \boldsymbol{\omega}_2 \cdot (\mathbb{I} - \hat{\mathbf{n}}_1 \hat{\mathbf{n}}_1) \cdot \boldsymbol{\omega}_2 + 2h(\hat{\boldsymbol{\varepsilon}}_\perp) (\mathbf{v}_Q - \mathbf{v}_P) \cdot \dot{\mathbf{H}}_1 \cdot \hat{\mathbf{n}}_1 \\ & + 2h(\hat{\boldsymbol{\varepsilon}}_\perp) (\mathbf{v}_Q - \mathbf{v}_P) \cdot \mathbf{H}_1 \cdot (\boldsymbol{\omega}_2 \times \hat{\mathbf{n}}_1) + (\dot{\boldsymbol{\omega}}_2 \times \hat{\boldsymbol{\varepsilon}}_\perp) \cdot \mathbf{H}_1 \cdot \hat{\boldsymbol{\varepsilon}}_\perp \\ & - \hat{\boldsymbol{\varepsilon}}_\perp \cdot [(\boldsymbol{\omega}_2^2 \mathbb{I} - \boldsymbol{\omega}_2 \boldsymbol{\omega}_2) \cdot \mathbf{H}_1] \cdot \hat{\boldsymbol{\varepsilon}}_\perp + 2(\boldsymbol{\omega}_2 \times \hat{\boldsymbol{\varepsilon}}_\perp) \cdot \dot{\mathbf{H}}_1 \cdot \hat{\boldsymbol{\varepsilon}}_\perp \\ & + (\boldsymbol{\omega}_2 \times \hat{\boldsymbol{\varepsilon}}_\perp) \cdot \mathbf{H}_1 \cdot (\boldsymbol{\omega}_2 \times \hat{\boldsymbol{\varepsilon}}_\perp) + h(\hat{\boldsymbol{\varepsilon}}_\perp) \hat{\mathbf{n}}_1 \cdot \ddot{\mathbf{H}}_1 \cdot \hat{\boldsymbol{\varepsilon}}_\perp + \frac{1}{2} \hat{\boldsymbol{\varepsilon}}_\perp \cdot \ddot{\mathbf{H}}_1 \cdot \hat{\boldsymbol{\varepsilon}}_\perp, \end{aligned} \quad (106)$$

$$\begin{aligned} a_{3\varepsilon} = & h(\hat{\boldsymbol{\varepsilon}}_\perp)(\dot{\boldsymbol{\omega}}_2 \times \hat{\mathbf{n}}_1) + h(\hat{\boldsymbol{\varepsilon}}_\perp)(\boldsymbol{\omega}_2 \cdot \hat{\mathbf{n}}_1) \boldsymbol{\omega}_2 \cdot \mathbf{H}_1 \cdot \hat{\boldsymbol{\varepsilon}}_\perp \\ & + 2h(\hat{\boldsymbol{\varepsilon}}_\perp)(\boldsymbol{\omega}_2 \times \hat{\boldsymbol{\varepsilon}}_\perp) \cdot \dot{\mathbf{H}}_1 \cdot \hat{\mathbf{n}}_1 + 2h(\hat{\boldsymbol{\varepsilon}}_\perp)(\boldsymbol{\omega}_2 \times \hat{\mathbf{n}}_1) \cdot \dot{\mathbf{H}}_1 \cdot \hat{\boldsymbol{\varepsilon}}_\perp \\ & + h(\hat{\boldsymbol{\varepsilon}}_\perp) \hat{\mathbf{n}}_1 \cdot \ddot{\mathbf{H}}_1 \cdot \hat{\boldsymbol{\varepsilon}}_\perp, \end{aligned} \quad (107)$$

$$\begin{aligned} a_{4\varepsilon} = & 2h^2(\hat{\boldsymbol{\varepsilon}}_\perp)(\boldsymbol{\omega}_2 \times \hat{\mathbf{n}}_1) \cdot \dot{\mathbf{H}}_1 \cdot \hat{\mathbf{n}}_1 + h^2(\hat{\boldsymbol{\varepsilon}}_\perp)(\boldsymbol{\omega}_2 \times \hat{\mathbf{n}}_1) \cdot \mathbf{H}_1 \cdot (\boldsymbol{\omega}_2 \times \hat{\mathbf{n}}_1) \\ & + \frac{1}{2} h^2(\hat{\boldsymbol{\varepsilon}}_\perp) \hat{\mathbf{n}}_1 \cdot \ddot{\mathbf{H}}_1 \cdot \hat{\mathbf{n}}_1, \end{aligned} \quad (108)$$

for the neighboring points.

$$h(\hat{\boldsymbol{\varepsilon}}_\perp) = \frac{1}{2} \hat{\boldsymbol{\varepsilon}}_\perp \cdot \mathbf{H}_2 \cdot \hat{\boldsymbol{\varepsilon}}_\perp. \quad (109)$$

6.3 Part III - Information to Satisfy Completeness

6.4 Describing the motion

Here we look at the coefficients in the Taylor series expansion of the positions of points on the two bodies as functions of time.

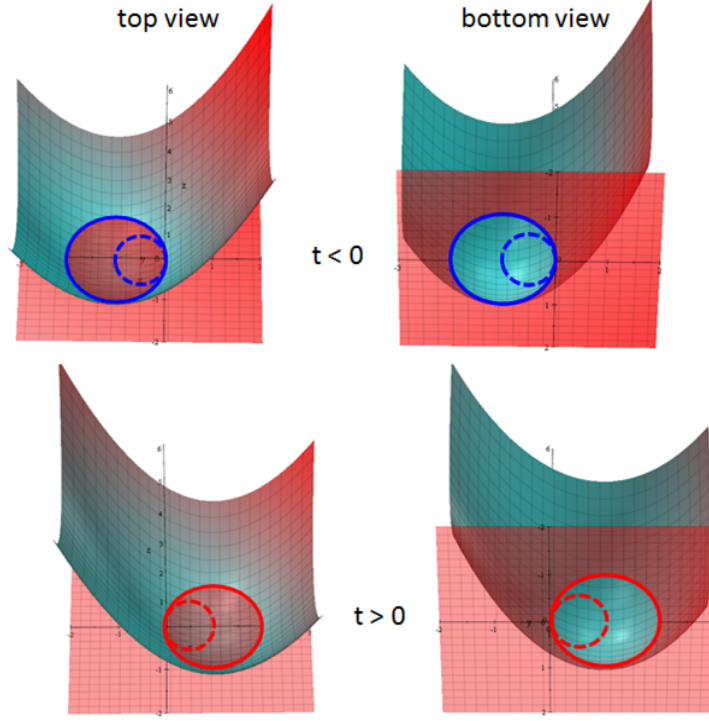


Figure 7: Illustration of the Figure of eight pattern from different perspectives and at different times.

The bodies are moving with constant linear and angular momentum, conserving kinetic energy. If the position of a point on the surface of one body is $\mathbf{r}(t)$, then we have for the instantaneous velocity

$$\begin{aligned}\dot{\mathbf{r}} &= \dot{\mathbf{r}}_c + \boldsymbol{\omega} \times (\mathbf{r} - \mathbf{r}_c) \\ &= \dot{\mathbf{r}}_c + \boldsymbol{\omega} \times \boldsymbol{\rho},\end{aligned}\tag{110}$$

where $\boldsymbol{\rho} = \mathbf{r} - \mathbf{r}_c$ is a body fixed vector, from the center of mass of the particle to the point in question on the body. Continuing, we have for the instantaneous acceleration

$$\begin{aligned}\ddot{\mathbf{r}} &= \dot{\boldsymbol{\omega}} \times \boldsymbol{\rho} + \boldsymbol{\omega} \times \dot{\boldsymbol{\rho}} \\ &= \dot{\boldsymbol{\omega}} \times \boldsymbol{\rho} + \boldsymbol{\omega} \times (\boldsymbol{\omega} \times \boldsymbol{\rho}) \\ &= \dot{\boldsymbol{\omega}} \times \boldsymbol{\rho} + (\boldsymbol{\omega} \cdot \boldsymbol{\rho})\boldsymbol{\omega} - \omega^2 \boldsymbol{\rho}.\end{aligned}\tag{111}$$

We note that $\dot{\mathbf{r}}_c = 0$ due to linear momentum conservation. Angular momentum conservation gives (Euler's equations in the lab frame),

$$\dot{\boldsymbol{\omega}} = -\mathbf{I}^{-1} \cdot (\boldsymbol{\omega} \times \mathbf{I} \cdot \boldsymbol{\omega}),\tag{112}$$

where \mathbf{I} is the moment of inertia tensor, and⁵

$$\dot{\mathbf{I}} = \boldsymbol{\omega} \times \mathbf{I} - \mathbf{I} \times \boldsymbol{\omega}. \quad (113)$$

Substitution gives

$$\ddot{\mathbf{r}} = -\mathbf{I}^{-1} \cdot (\boldsymbol{\omega} \times \mathbf{I} \cdot \boldsymbol{\omega}) \times \boldsymbol{\rho} + \boldsymbol{\omega}(\boldsymbol{\omega} \cdot \boldsymbol{\rho}) - \omega^2 \boldsymbol{\rho}, \quad (114)$$

and

$$(\mathbf{I}^{-1})^\cdot = -\mathbf{I}^{-1} \dot{\mathbf{I}} \mathbf{I}^{-1}, \quad (115)$$

or

$$(\mathbf{I}^{-1})^\cdot = \boldsymbol{\omega} \times \mathbf{I}^{-1} - \mathbf{I}^{-1} \times \boldsymbol{\omega}. \quad (116)$$

Continuing gives the instantaneous jerk

$$\begin{aligned} \ddot{\mathbf{r}} &= \ddot{\boldsymbol{\omega}} \times \boldsymbol{\rho} + 2\dot{\boldsymbol{\omega}} \times \dot{\boldsymbol{\rho}} + \boldsymbol{\omega} \times \ddot{\boldsymbol{\rho}} \\ &= \ddot{\boldsymbol{\omega}} \times \boldsymbol{\rho} + 2(\dot{\boldsymbol{\omega}} \cdot \boldsymbol{\rho})\boldsymbol{\omega} - 3(\dot{\boldsymbol{\omega}} \cdot \boldsymbol{\omega})\boldsymbol{\rho} + (\boldsymbol{\omega} \cdot \boldsymbol{\rho})\dot{\boldsymbol{\omega}} - \omega^2 \boldsymbol{\omega} \times \boldsymbol{\rho}, \end{aligned} \quad (117)$$

where, by Eq. (112),

$$\ddot{\boldsymbol{\omega}} = -(\mathbf{I}^{-1})^\cdot \cdot (\boldsymbol{\omega} \times \mathbf{I} \cdot \boldsymbol{\omega}) - \mathbf{I}^{-1} \cdot (\dot{\boldsymbol{\omega}} \times \mathbf{I} \cdot \boldsymbol{\omega}) - \mathbf{I}^{-1} \cdot (\boldsymbol{\omega} \times \dot{\mathbf{I}} \cdot \boldsymbol{\omega}) - \mathbf{I}^{-1} \cdot (\boldsymbol{\omega} \times \mathbf{I} \cdot \dot{\boldsymbol{\omega}}), \quad (118)$$

and $\dot{\boldsymbol{\omega}}$ and $\dot{\mathbf{I}}$ are given by Eqs. (112) and (113) respectively. By substitution into Eq. (117), we have an explicit expression for the jerk.

6.4.1 Kinetic Equations

The main equation can be derived at once from first principles.

$$\begin{aligned} F_1(t, \mathbf{r}_{Q+}(t)) &= (\hat{\mathbf{n}}_1 \cdot \boldsymbol{\delta}_Q + \frac{1}{2} \boldsymbol{\delta}_Q \cdot \mathbf{H}_1 \cdot \boldsymbol{\delta}_Q) \Big|_{t=0} \\ &\quad + \frac{\partial}{\partial t} (\hat{\mathbf{n}}_1 \cdot \boldsymbol{\delta}_Q + \frac{1}{2} \boldsymbol{\delta}_Q \cdot \mathbf{H}_1 \cdot \boldsymbol{\delta}_Q) \Big|_{t=0} t \\ &\quad + \frac{1}{2} \frac{\partial^2}{\partial t^2} (\hat{\mathbf{n}}_1 \cdot \boldsymbol{\delta}_Q + \frac{1}{2} \boldsymbol{\delta}_Q \cdot \mathbf{H}_1 \cdot \boldsymbol{\delta}_Q) \Big|_{t=0} t^2 + O(\max(|\boldsymbol{\delta}_Q|^3, t^3)). \end{aligned} \quad (119)$$

⁵In Cartesian components, the rhs of Eq. (113) would read $\varepsilon_{\alpha\beta\gamma}\omega_\beta I_{\gamma\delta} - I_{\alpha\beta}\omega_\gamma \varepsilon_{\delta\beta\gamma}$.

Then

$$\begin{aligned}
F_1(t, \mathbf{r}_Q(t)) &= (\hat{\mathbf{n}}_1 \cdot \boldsymbol{\delta}_Q + \frac{1}{2} \boldsymbol{\delta}_Q \cdot \mathbf{H}_1 \cdot \boldsymbol{\delta}_Q) \Big|_{t=0} \\
&\quad + (\dot{\hat{\mathbf{n}}}_1 \cdot \boldsymbol{\delta}_Q + \hat{\mathbf{n}}_1 \cdot \dot{\boldsymbol{\delta}}_Q + \dot{\boldsymbol{\delta}}_Q \cdot \mathbf{H}_1 \cdot \boldsymbol{\delta}_Q + \frac{1}{2} \boldsymbol{\delta}_Q \cdot \dot{\mathbf{H}}_1 \cdot \boldsymbol{\delta}_Q) \Big|_{t=0} t \\
&\quad + \frac{1}{2} (\ddot{\hat{\mathbf{n}}}_1 \cdot \boldsymbol{\delta}_Q + 2\dot{\hat{\mathbf{n}}}_1 \cdot \dot{\boldsymbol{\delta}}_Q + \hat{\mathbf{n}}_1 \cdot \ddot{\boldsymbol{\delta}}_Q \\
&\quad + \ddot{\boldsymbol{\delta}}_Q \cdot \mathbf{H}_1 \cdot \boldsymbol{\delta}_Q + 2\dot{\boldsymbol{\delta}}_Q \cdot \dot{\mathbf{H}}_1 \cdot \boldsymbol{\delta}_Q + \dot{\boldsymbol{\delta}}_Q \cdot \mathbf{H}_1 \cdot \dot{\boldsymbol{\delta}}_Q \\
&\quad + \frac{1}{2} \boldsymbol{\delta}_Q \cdot \ddot{\mathbf{H}}_1 \cdot \boldsymbol{\delta}_Q) \Big|_{t=0} t^2 + O(\max(|\boldsymbol{\delta}_Q|^3, t^3)). \tag{120}
\end{aligned}$$

Now

$$\boldsymbol{\delta}_Q = (\mathbf{r}_Q - \mathbf{r}_P) + \boldsymbol{\varepsilon}_Q, \tag{121}$$

and substitution gives

$$\begin{aligned}
F_1 &= (\hat{\mathbf{n}}_1 \cdot (\mathbf{v}_Q - \mathbf{v}_P)) t \\
&\quad + \frac{1}{2} (2\dot{\hat{\mathbf{n}}}_1 \cdot (\mathbf{v}_Q - \mathbf{v}_P) + \hat{\mathbf{n}}_1 \cdot (\dot{\mathbf{v}}_Q - \dot{\mathbf{v}}_P) + (\mathbf{v}_Q - \mathbf{v}_P) \cdot \mathbf{H}_1 \cdot (\mathbf{v}_Q - \mathbf{v}_P)) t^2 \\
&\quad + ((\mathbf{v}_Q - \mathbf{v}_P) \cdot \mathbf{H}_1 \cdot \boldsymbol{\varepsilon}_Q) t \\
&\quad + \frac{1}{2} ((\dot{\mathbf{v}}_Q - \dot{\mathbf{v}}_P) \cdot \mathbf{H}_1 \cdot \boldsymbol{\varepsilon}_Q + 2(\mathbf{v}_Q - \mathbf{v}_P) \cdot \dot{\mathbf{H}}_1 \cdot \boldsymbol{\varepsilon}_Q + 2(\mathbf{v}_Q - \mathbf{v}_P) \cdot \mathbf{H}_1 \cdot \dot{\boldsymbol{\varepsilon}}_Q) t^2 \\
&\quad + (\hat{\mathbf{n}}_1 \cdot \boldsymbol{\varepsilon}_Q + \frac{1}{2} \boldsymbol{\varepsilon}_Q \cdot \mathbf{H}_1 \cdot \boldsymbol{\varepsilon}_Q) \\
&\quad + (\dot{\hat{\mathbf{n}}}_1 \cdot \boldsymbol{\varepsilon}_Q + \hat{\mathbf{n}}_1 \cdot \dot{\boldsymbol{\varepsilon}}_Q + \dot{\boldsymbol{\varepsilon}}_Q \cdot \mathbf{H}_1 \cdot \boldsymbol{\varepsilon}_Q + \frac{1}{2} \boldsymbol{\varepsilon}_Q \cdot \dot{\mathbf{H}}_1 \cdot \boldsymbol{\varepsilon}_Q) t \\
&\quad + \frac{1}{2} (\ddot{\hat{\mathbf{n}}}_1 \cdot \boldsymbol{\varepsilon}_Q + 2\dot{\hat{\mathbf{n}}}_1 \cdot \dot{\boldsymbol{\varepsilon}}_Q + \hat{\mathbf{n}}_1 \cdot \ddot{\boldsymbol{\varepsilon}}_Q \\
&\quad + \ddot{\boldsymbol{\varepsilon}}_Q \cdot \mathbf{H}_1 \cdot \boldsymbol{\varepsilon}_Q + 2\dot{\boldsymbol{\varepsilon}}_Q \cdot \dot{\mathbf{H}}_1 \cdot \boldsymbol{\varepsilon}_Q + \dot{\boldsymbol{\varepsilon}}_Q \cdot \mathbf{H}_1 \cdot \dot{\boldsymbol{\varepsilon}}_Q + \frac{1}{2} \boldsymbol{\varepsilon}_Q \cdot \ddot{\mathbf{H}}_1 \cdot \boldsymbol{\varepsilon}_Q) t^2 + O(\max(|\boldsymbol{\delta}_Q|^3, t^3)) \tag{122}
\end{aligned}$$

or

$$\begin{aligned}
F_1 &= (\hat{\mathbf{n}}_1 \cdot (\mathbf{v}_Q - \mathbf{v}_P)) \Big|_{t=0} t \\
&\quad + \frac{1}{2} (2\dot{\hat{\mathbf{n}}}_1 \cdot (\mathbf{v}_Q - \mathbf{v}_P) + \hat{\mathbf{n}}_1 \cdot (\dot{\mathbf{v}}_Q - \dot{\mathbf{v}}_P) \\
&\quad + (\mathbf{v}_Q - \mathbf{v}_P) \cdot \mathbf{H}_1 \cdot (\mathbf{v}_Q - \mathbf{v}_P)) \Big|_{t=0} t^2 \\
&\quad + (\hat{\mathbf{n}}_1 \cdot \boldsymbol{\varepsilon}_Q + \frac{1}{2} \boldsymbol{\varepsilon}_Q \cdot \mathbf{H}_1 \cdot \boldsymbol{\varepsilon}_Q) \Big|_{t=0} \\
&\quad + (\dot{\hat{\mathbf{n}}}_1 \cdot \boldsymbol{\varepsilon}_Q + \hat{\mathbf{n}}_1 \cdot \dot{\boldsymbol{\varepsilon}}_Q + (\mathbf{v}_Q - \mathbf{v}_P) \cdot \mathbf{H}_1 \cdot \boldsymbol{\varepsilon}_Q + \dot{\boldsymbol{\varepsilon}}_Q \cdot \mathbf{H}_1 \cdot \boldsymbol{\varepsilon}_Q + \frac{1}{2} \boldsymbol{\varepsilon}_Q \cdot \dot{\mathbf{H}}_1 \cdot \boldsymbol{\varepsilon}_Q) \Big|_{t=0} t \\
&\quad + \frac{1}{2} (\ddot{\hat{\mathbf{n}}}_1 \cdot \boldsymbol{\varepsilon}_Q + 2\dot{\hat{\mathbf{n}}}_1 \cdot \dot{\boldsymbol{\varepsilon}}_Q + \hat{\mathbf{n}}_1 \cdot \ddot{\boldsymbol{\varepsilon}}_Q + \\
&\quad + (\dot{\mathbf{v}}_Q - \dot{\mathbf{v}}_P) \cdot \mathbf{H}_1 \cdot \boldsymbol{\varepsilon}_Q + 2(\mathbf{v}_Q - \mathbf{v}_P) \cdot \dot{\mathbf{H}}_1 \cdot \boldsymbol{\varepsilon}_Q + 2(\mathbf{v}_Q - \mathbf{v}_P) \cdot \mathbf{H}_1 \cdot \dot{\boldsymbol{\varepsilon}}_Q \\
&\quad + \ddot{\boldsymbol{\varepsilon}}_Q \cdot \mathbf{H}_1 \cdot \boldsymbol{\varepsilon}_Q + 2\dot{\boldsymbol{\varepsilon}}_Q \cdot \dot{\mathbf{H}}_1 \cdot \boldsymbol{\varepsilon}_Q + \dot{\boldsymbol{\varepsilon}}_Q \cdot \mathbf{H}_1 \cdot \dot{\boldsymbol{\varepsilon}}_Q + \frac{1}{2} \boldsymbol{\varepsilon}_Q \cdot \ddot{\mathbf{H}}_1 \cdot \boldsymbol{\varepsilon}_Q) \Big|_{t=0} t^2 + O(\max(|\boldsymbol{\delta}_Q|^3, t^3)) \tag{123}
\end{aligned}$$

6.5 Part IV: Proofs of selected claims

6.5.1 Proof of $a_P - (\frac{v_{\varepsilon P}^2}{2x_{2\varepsilon P}})_{\max} = a_Q - (\frac{v_{\varepsilon Q}^2}{2x_{2\varepsilon Q}})_{\max}$

From previous analysis, for potentially most deeply penetrating neighboring point on body 2, we have

$$F_1(\mathbf{r}_{Q+}(t), t) = v_Q t + \frac{1}{2}(a_Q - \frac{v_{\varepsilon Q}^2}{x_{2\varepsilon Q}})t^2 + O_\varepsilon(t^3), \quad (124)$$

where

$$v_Q = \hat{\mathbf{n}}_2 \cdot (\mathbf{v}_Q - \mathbf{v}_P), \quad (125)$$

$$\begin{aligned} a_Q &= 2(\boldsymbol{\omega}_1 \times \hat{\mathbf{n}}_1) \cdot (\mathbf{v}_Q - \mathbf{v}_P) + \hat{\mathbf{n}}_1 \cdot (\dot{\mathbf{v}}_Q - \dot{\mathbf{v}}_P) + (\mathbf{v}_Q - \mathbf{v}_P) \cdot \mathbf{H}_1 \cdot (\mathbf{v}_Q - \mathbf{v}_P) \\ &= -\hat{\mathbf{n}}_1 \times (\boldsymbol{\omega}_1 + \boldsymbol{\omega}_2) \cdot (\mathbf{v}_Q - \mathbf{v}_P) + \hat{\mathbf{n}}_1 \cdot (\dot{\mathbf{v}}_Q - \dot{\mathbf{v}}_P) \\ &\quad + \hat{\mathbf{n}}_1 \times (\boldsymbol{\omega}_2 - \boldsymbol{\omega}_1) \cdot (\mathbf{v}_Q - \mathbf{v}_P) + (\mathbf{v}_Q - \mathbf{v}_P) \cdot \mathbf{H}_1 \cdot (\mathbf{v}_Q - \mathbf{v}_P), \end{aligned} \quad (126)$$

$$x_{2\varepsilon Q} = \frac{1}{2}(\hat{\boldsymbol{\varepsilon}}_\perp \cdot \mathbf{H}_2 \cdot \hat{\boldsymbol{\varepsilon}}_\perp) + \frac{1}{2}(\hat{\boldsymbol{\varepsilon}}_\perp \cdot \mathbf{H}_1 \cdot \hat{\boldsymbol{\varepsilon}}_\perp) = \frac{1}{2}\hat{\boldsymbol{\varepsilon}}_\perp (\mathbf{H}_2 + \mathbf{H}_1) \hat{\boldsymbol{\varepsilon}}_\perp, \quad (127)$$

$$v_{\varepsilon Q} = \hat{\mathbf{n}}_1 \times (\boldsymbol{\omega}_2 - \boldsymbol{\omega}_1) \cdot \hat{\boldsymbol{\varepsilon}}_\perp + (\mathbf{v}_Q - \mathbf{v}_P) \cdot \mathbf{H}_1 \cdot \hat{\boldsymbol{\varepsilon}}_\perp. \quad (128)$$

The maximum of $\frac{v_{\varepsilon Q}^2}{2x_{2\varepsilon Q}}$ is obtained at the direction

$$\hat{\boldsymbol{\varepsilon}}_{\perp Q}^* = \frac{(\mathbf{H}_2 + \mathbf{H}_1)^{-1} \cdot (\hat{\mathbf{n}}_1 \times (\boldsymbol{\omega}_2 - \boldsymbol{\omega}_1) + \mathbf{H}_1 \cdot (\mathbf{v}_Q - \mathbf{v}_P))}{|(\mathbf{H}_2 + \mathbf{H}_1)^{-1} \cdot (\hat{\mathbf{n}}_1 \times (\boldsymbol{\omega}_2 - \boldsymbol{\omega}_1) + \mathbf{H}_1 \cdot (\mathbf{v}_Q - \mathbf{v}_P))|}. \quad (129)$$

To make our presentation simpler, we denote

$$L_{Q^*} = |(\mathbf{H}_2 + \mathbf{H}_1)^{-1} \cdot (\hat{\mathbf{n}}_1 \times (\boldsymbol{\omega}_2 - \boldsymbol{\omega}_1) + \mathbf{H}_1 \cdot (\mathbf{v}_Q - \mathbf{v}_P))|. \quad (130)$$

Then direct substitution of $\hat{\boldsymbol{\varepsilon}}_{\perp Q}^*$ gives

$$v_{\varepsilon Q}^* = (\hat{\mathbf{n}}_1 \times (\boldsymbol{\omega}_2 - \boldsymbol{\omega}_1) + (\mathbf{v}_Q - \mathbf{v}_P) \cdot \mathbf{H}_1) \cdot \hat{\boldsymbol{\varepsilon}}_{\perp Q}^* = L_{Q^*} 2x_{2\varepsilon Q}^*, \quad (131)$$

and this far in this part

$$\begin{aligned}
& (2a_Q x_{2\varepsilon Q} - v_{\varepsilon Q}^2)(\hat{\varepsilon}_\perp^*) \\
= & (2(\boldsymbol{\omega}_1 \times \hat{\mathbf{n}}_1) \cdot (\mathbf{v}_Q - \mathbf{v}_P) + \hat{\mathbf{n}}_1 \cdot (\dot{\mathbf{v}}_Q - \dot{\mathbf{v}}_P) + (\mathbf{v}_Q - \mathbf{v}_P) \cdot \mathbf{H}_1 \cdot (\mathbf{v}_Q - \mathbf{v}_P))v_{\varepsilon Q}^*/L_{Q^*} - v_{\varepsilon Q}^{*2} \\
= & v_{\varepsilon Q}^*/L_{Q^*}[(-(\hat{\mathbf{n}}_1 \times (\boldsymbol{\omega}_1 + \boldsymbol{\omega}_2)) \cdot (\mathbf{v}_Q - \mathbf{v}_P) + \hat{\mathbf{n}}_1 \cdot (\dot{\mathbf{v}}_Q - \dot{\mathbf{v}}_P) \\
& + \hat{\mathbf{n}}_1 \times (\boldsymbol{\omega}_2 - \boldsymbol{\omega}_1) \cdot (\mathbf{v}_Q - \mathbf{v}_P) + (\mathbf{v}_Q - \mathbf{v}_P) \cdot \mathbf{H}_1 \cdot (\mathbf{v}_Q - \mathbf{v}_P)) - v_{\varepsilon Q}^* L_{Q^*}] \\
= & v_{\varepsilon Q}^*/L_{Q^*}[(-(\hat{\mathbf{n}}_1 \times (\boldsymbol{\omega}_1 + \boldsymbol{\omega}_2)) \cdot (\mathbf{v}_Q - \mathbf{v}_P) + \hat{\mathbf{n}}_1 \cdot (\dot{\mathbf{v}}_Q - \dot{\mathbf{v}}_P)] \\
& + v_{\varepsilon Q}^*/L_{Q^*}[(\hat{\mathbf{n}}_1 \times (\boldsymbol{\omega}_2 - \boldsymbol{\omega}_1) + \mathbf{H}_1 \cdot (\mathbf{v}_Q - \mathbf{v}_P)) \\
& \cdot ((\mathbf{v}_Q - \mathbf{v}_P) - (\mathbf{H}_2 + \mathbf{H}_1)^{-1} \cdot (\hat{\mathbf{n}}_1 \times (\boldsymbol{\omega}_2 - \boldsymbol{\omega}_1) + \mathbf{H}_1 \cdot (\mathbf{v}_Q - \mathbf{v}_P)))] \\
= & 2x_{2\varepsilon Q}^*[(-(\hat{\mathbf{n}}_1 \times (\boldsymbol{\omega}_1 + \boldsymbol{\omega}_2)) \cdot (\mathbf{v}_Q - \mathbf{v}_P) + \hat{\mathbf{n}}_1 \cdot (\dot{\mathbf{v}}_Q - \dot{\mathbf{v}}_P) \\
& + (\hat{\mathbf{n}}_1 \times (\boldsymbol{\omega}_2 - \boldsymbol{\omega}_1) + \mathbf{H}_1 \cdot (\mathbf{v}_Q - \mathbf{v}_P)) \\
& \cdot ((\mathbf{v}_Q - \mathbf{v}_P) - (\mathbf{H}_2 + \mathbf{H}_1)^{-1} \cdot (\hat{\mathbf{n}}_1 \times (\boldsymbol{\omega}_2 - \boldsymbol{\omega}_1) + \mathbf{H}_1 \cdot (\mathbf{v}_Q - \mathbf{v}_P)))] . \tag{132}
\end{aligned}$$

Similarly, for potentially most deeply penetrating neighboring point on body 1, we have

$$F_2(\mathbf{r}_{P+}(t), t) = v_P t + \frac{1}{2}(a_P - \frac{v_{\varepsilon P}^2}{x_{2\varepsilon P}})t^2 + O_\varepsilon(t^3), \tag{133}$$

where

$$v_P = \hat{\mathbf{n}}_2 \cdot (\mathbf{v}_P - \mathbf{v}_Q), \tag{134}$$

$$a_P = 2(\boldsymbol{\omega}_2 \times \hat{\mathbf{n}}_2) \cdot (\mathbf{v}_P - \mathbf{v}_Q) + \hat{\mathbf{n}}_2 \cdot (\dot{\mathbf{v}}_P - \dot{\mathbf{v}}_Q) + (\mathbf{v}_P - \mathbf{v}_Q) \cdot \mathbf{H}_2 \cdot (\mathbf{v}_P - \mathbf{v}_Q), \tag{135}$$

$$x_{2\varepsilon P} = \frac{1}{2}(\hat{\varepsilon}_\perp \cdot \mathbf{H}_1 \cdot \hat{\varepsilon}_\perp) + \frac{1}{2}(\hat{\varepsilon}_\perp \cdot \mathbf{H}_2 \cdot \hat{\varepsilon}_\perp), \tag{136}$$

$$v_{\varepsilon P} = \hat{\mathbf{n}}_2 \times (\boldsymbol{\omega}_1 - \boldsymbol{\omega}_2) \cdot \hat{\varepsilon}_\perp + (\mathbf{v}_P - \mathbf{v}_Q) \cdot \mathbf{H}_2 \cdot \varepsilon_\perp, \tag{137}$$

The maximum of $\frac{v_{\varepsilon P}^2}{2x_{2\varepsilon P}}$ is obtained in the direction

$$\hat{\varepsilon}_{\perp P}^* = \frac{(\mathbf{H}_2 + \mathbf{H}_1)^{-1} \cdot (\hat{\mathbf{n}}_2 \times (\boldsymbol{\omega}_1 - \boldsymbol{\omega}_2) + \mathbf{H}_2 \cdot (\mathbf{v}_P - \mathbf{v}_Q))}{|(\mathbf{H}_2 + \mathbf{H}_1)^{-1} \cdot (\hat{\mathbf{n}}_2 \times (\boldsymbol{\omega}_1 - \boldsymbol{\omega}_2) + \mathbf{H}_2 \cdot (\mathbf{v}_P - \mathbf{v}_Q))|}. \tag{138}$$

We denote

$$L_{P^*} = |((\mathbf{H}_2 + \mathbf{H}_1)^{-1} \cdot (\hat{\mathbf{n}}_2 \times (\boldsymbol{\omega}_1 - \boldsymbol{\omega}_2) + \mathbf{H}_2 \cdot (\mathbf{v}_P - \mathbf{v}_Q))|, \tag{139}$$

$$v_{\varepsilon P}^* = (\hat{\mathbf{n}}_2 \times (\boldsymbol{\omega}_1 - \boldsymbol{\omega}_2) + (\mathbf{v}_P - \mathbf{v}_Q) \cdot \mathbf{H}_2) \cdot \hat{\varepsilon}_{\perp P}^* = L_{P^*} 2x_{2\varepsilon P}^*. \tag{140}$$

Using the fact that

$$\hat{\mathbf{n}}_2 = -\hat{\mathbf{n}}_1, \tag{141}$$

we have

$$\begin{aligned}
& (2a_P x_{2\varepsilon P} - v_{\varepsilon P}^2)(\hat{\boldsymbol{\varepsilon}}_{\perp}^*) \\
= & v_{\varepsilon P}^*/L_{P^*} [((\hat{\mathbf{n}}_2 \times (\boldsymbol{\omega}_1 + \boldsymbol{\omega}_2)) \cdot (\mathbf{v}_Q - \mathbf{v}_P) - \hat{\mathbf{n}}_2 \cdot (\dot{\mathbf{v}}_Q - \dot{\mathbf{v}}_P)] \\
& + v_{\varepsilon P}^*/L_{P^*} [(-\hat{\mathbf{n}}_2 \times (\boldsymbol{\omega}_2 - \boldsymbol{\omega}_1) - \mathbf{H}_2 \cdot (\mathbf{v}_Q - \mathbf{v}_P)) \\
& \cdot (-(\mathbf{v}_Q - \mathbf{v}_P) - (\mathbf{H}_2 + \mathbf{H}_1)^{-1} \cdot (-\hat{\mathbf{n}}_2 \times (\boldsymbol{\omega}_2 - \boldsymbol{\omega}_1) - \mathbf{H}_2 \cdot (\mathbf{v}_Q - \mathbf{v}_P))] \\
= & v_{\varepsilon P}^*/L_{P^*} [((-\hat{\mathbf{n}}_1 \times (\boldsymbol{\omega}_1 + \boldsymbol{\omega}_2)) \cdot (\mathbf{v}_Q - \mathbf{v}_P) + \hat{\mathbf{n}}_1 \cdot (\dot{\mathbf{v}}_Q - \dot{\mathbf{v}}_P)] \\
& + v_{\varepsilon P}^*/L_{P^*} [(\hat{\mathbf{n}}_1 \times (\boldsymbol{\omega}_2 - \boldsymbol{\omega}_1) - \mathbf{H}_2 \cdot (\mathbf{v}_Q - \mathbf{v}_P)) \\
& \cdot (-(\mathbf{v}_Q - \mathbf{v}_P) - (\mathbf{H}_2 + \mathbf{H}_1)^{-1} \cdot (\hat{\mathbf{n}}_1 \times (\boldsymbol{\omega}_2 - \boldsymbol{\omega}_1) - \mathbf{H}_2 \cdot (\mathbf{v}_Q - \mathbf{v}_P))] \\
= & 2x_{2\varepsilon P}^* [((-\hat{\mathbf{n}}_1 \times (\boldsymbol{\omega}_1 + \boldsymbol{\omega}_2)) \cdot (\mathbf{v}_Q - \mathbf{v}_P) + \hat{\mathbf{n}}_1 \cdot (\dot{\mathbf{v}}_Q - \dot{\mathbf{v}}_P) \\
& + (\hat{\mathbf{n}}_1 \times (\boldsymbol{\omega}_2 - \boldsymbol{\omega}_1) - \mathbf{H}_2 \cdot (\mathbf{v}_Q - \mathbf{v}_P)) \\
& \cdot (-(\mathbf{v}_Q - \mathbf{v}_P) - (\mathbf{H}_2 + \mathbf{H}_1)^{-1} \cdot (\hat{\mathbf{n}}_1 \times (\boldsymbol{\omega}_2 - \boldsymbol{\omega}_1) - \mathbf{H}_2 \cdot (\mathbf{v}_Q - \mathbf{v}_P))]. \tag{142}
\end{aligned}$$

Using the fact that

$$\mathbf{H}_2 \cdot (\mathbf{H}_2 + \mathbf{H}_1)^{-1} = \mathbf{I} - \mathbf{H}_1 \cdot (\mathbf{H}_2 + \mathbf{H}_1)^{-1}, \tag{143}$$

the above expression, can be shown to be, via straightforward calculation,

$$\begin{aligned}
& (2a_P x_{2\varepsilon P} - v_{\varepsilon P}^2)(\hat{\boldsymbol{\varepsilon}}_{\perp}^*) \\
= & 2x_{2\varepsilon P}^* [((-\hat{\mathbf{n}}_1 \times (\boldsymbol{\omega}_1 + \boldsymbol{\omega}_2)) \cdot (\mathbf{v}_Q - \mathbf{v}_P) + \hat{\mathbf{n}}_1 \cdot (\dot{\mathbf{v}}_Q - \dot{\mathbf{v}}_P) \\
& + (\hat{\mathbf{n}}_1 \times (\boldsymbol{\omega}_2 - \boldsymbol{\omega}_1) + \mathbf{H}_1 \cdot (\mathbf{v}_Q - \mathbf{v}_P)) \\
& \cdot ((\mathbf{v}_Q - \mathbf{v}_P) - (\mathbf{H}_2 + \mathbf{H}_1)^{-1} \cdot (\hat{\mathbf{n}}_1 \times (\boldsymbol{\omega}_2 - \boldsymbol{\omega}_1) + \mathbf{H}_1 \cdot (\mathbf{v}_Q - \mathbf{v}_P))]. \tag{144}
\end{aligned}$$

Thus

$$\frac{2a_P x_{2\varepsilon P}^* - v_{\varepsilon P}^{*2}}{2x_{2\varepsilon P}^*} = \frac{2a_Q x_{2\varepsilon Q}^* - v_{\varepsilon Q}^{*2}}{x_{2\varepsilon Q}^*}, \tag{145}$$

or

$$a_P - \left(\frac{v_{\varepsilon P}^2}{2x_{2\varepsilon P}}\right)_{\max} = a_Q - \left(\frac{v_{\varepsilon Q}^2}{2x_{2\varepsilon Q}}\right)_{\max}, \tag{146}$$

which indicates that the terms $a_P - \left(\frac{v_{\varepsilon P}^2}{2x_{2\varepsilon P}}\right)_{\max}$ and $a_Q - \left(\frac{v_{\varepsilon Q}^2}{2x_{2\varepsilon Q}}\right)_{\max}$ will be positive, zero, or negative simultaneously.

6.5.2 Proof of $\mathbf{a}_P \cdot \mathbf{n} < 0$ for a uniform ellipsoid

Here we compute the normal acceleration of a point on the boundary of a freely moving ellipsoidal body. The equation of the surface is given by

$$\mathbf{p} \cdot \mathbf{A} \cdot \mathbf{p} = 1, \quad (147)$$

where $\mathbf{p} = p_x \hat{\mathbf{x}} + p_y \hat{\mathbf{y}} + p_z \hat{\mathbf{z}}$ is the vector from the center of mass to a point \mathbf{p} on the surface, and

$$\mathbf{A} = \begin{bmatrix} \frac{1}{a^2} & 0 & 0 \\ 0 & \frac{1}{b^2} & 0 \\ 0 & 0 & \frac{1}{c^2} \end{bmatrix}, \quad (148)$$

where a, b, c are the semi-major axes lengths.

The acceleration of a point on the surface of the ellipsoid is given by

$$\mathbf{a}_P = \dot{\boldsymbol{\omega}} \times \mathbf{p} + \boldsymbol{\omega}(\boldsymbol{\omega} \cdot \mathbf{p}) - \omega^2 \mathbf{p}, \quad (149)$$

where

$$\dot{\boldsymbol{\omega}} = -\mathbf{I}^{-1} \cdot (\boldsymbol{\omega} \times \mathbf{I} \cdot \boldsymbol{\omega}) \times \mathbf{p}. \quad (150)$$

It follows at once that the component of the acceleration \mathbf{a}_P in the $\hat{\mathbf{p}}$ direction is non-positive; that is

$$\mathbf{a}_P \cdot \hat{\mathbf{p}} = \omega^2 p ((\dot{\boldsymbol{\omega}} \cdot \hat{\mathbf{p}})^2 - 1) \leq 0. \quad (151)$$

We write

$$\mathbf{I} = \begin{bmatrix} \alpha & 0 & 0 \\ 0 & \beta & 0 \\ 0 & 0 & \gamma \end{bmatrix} \quad (152)$$

and

$$\mathbf{I}^{-1} = \begin{bmatrix} \frac{1}{\alpha} & 0 & 0 \\ 0 & \frac{1}{\beta} & 0 \\ 0 & 0 & \frac{1}{\gamma} \end{bmatrix}. \quad (153)$$

For an uniform ellipsoid

$$\alpha = \frac{1}{5} M (b^2 + c^2), \quad (154)$$

$$\beta = \frac{1}{5} M (a^2 + c^2), \quad (155)$$

$$\gamma = \frac{1}{5} M (a^2 + b^2). \quad (156)$$

A direct evaluation of $\dot{\boldsymbol{\omega}} = -\mathbf{I}^{-1} \cdot (\boldsymbol{\omega} \times \mathbf{I} \cdot \boldsymbol{\omega})$ gives

$$\dot{\omega}_x = \omega_y \omega_z \left(\frac{c^2 - b^2}{c^2 + b^2} \right), \quad (157)$$

$$\dot{\omega}_y = \omega_x \omega_z \left(\frac{a^2 - c^2}{a^2 + c^2} \right), \quad (158)$$

$$\dot{\omega}_z = \omega_x \omega_y \left(\frac{b^2 - a^2}{b^2 + a^2} \right), \quad (159)$$

We note that the normal \mathbf{n} of the ellipsoid at point P is given by

$$\mathbf{n} = \frac{p_x}{a^2} \hat{\mathbf{x}} + \frac{p_y}{b^2} \hat{\mathbf{y}} + \frac{p_z}{c^2} \hat{\mathbf{z}}. \quad (160)$$

We can write the normal acceleration as

$$\begin{aligned} \mathbf{a}_P \cdot \mathbf{n} &= (\dot{\boldsymbol{\omega}} \times \mathbf{p}) \cdot \mathbf{n} + \boldsymbol{\omega}(\boldsymbol{\omega} \cdot \mathbf{p}) \cdot \mathbf{n} - \omega^2 \mathbf{p} \cdot \mathbf{n} \\ &= (\dot{\omega}_y p_z - \dot{\omega}_z p_y) \frac{p_x}{a^2} + (\dot{\omega}_z p_x - \dot{\omega}_x p_z) \frac{p_y}{b^2} + (\dot{\omega}_x p_y - \dot{\omega}_y p_x) \frac{p_z}{c^2} \\ &\quad + (\omega_x p_x + \omega_y p_y + \omega_z p_z) \left(\omega_x \frac{p_x}{a^2} + \omega_y \frac{p_y}{b^2} + \omega_z \frac{p_z}{c^2} \right) \\ &\quad - (\omega_x^2 + \omega_y^2 + \omega_z^2) \left(\frac{p_x^2}{a^2} + \frac{p_y^2}{b^2} + \frac{p_z^2}{c^2} \right). \end{aligned} \quad (161)$$

Explicitly

$$\begin{aligned} \mathbf{a}_P \cdot \mathbf{n} &= \omega_x \omega_y p_x p_y \left(\left(\frac{1}{b^2} - \frac{1}{a^2} \right) \frac{b^2 - a^2}{b^2 + a^2} + \left(\frac{1}{b^2} + \frac{1}{a^2} \right) \right) \\ &\quad + \omega_x \omega_z p_x p_z \left(\left(\frac{1}{a^2} - \frac{1}{c^2} \right) \frac{a^2 - c^2}{a^2 + c^2} + \left(\frac{1}{a^2} + \frac{1}{c^2} \right) \right) \\ &\quad + \omega_y \omega_z p_y p_z \left(\left(\frac{1}{c^2} - \frac{1}{b^2} \right) \frac{c^2 - b^2}{c^2 + b^2} + \left(\frac{1}{a^2} + \frac{1}{c^2} \right) \right) \\ &\quad + \omega_x^2 p_x^2 \frac{1}{a^2} + \omega_y^2 p_y^2 \frac{1}{b^2} + \omega_z^2 p_z^2 \frac{1}{c^2} \\ &\quad - (\omega_x^2 + \omega_y^2 + \omega_z^2). \end{aligned} \quad (162)$$

We note that

$$\left(\frac{1}{b^2} - \frac{1}{a^2} \right) \frac{b^2 - a^2}{b^2 + a^2} + \left(\frac{1}{b^2} + \frac{1}{a^2} \right) = \frac{4}{(a^2 + b^2)} \leq \frac{2}{ab}, \quad (163)$$

thus

$$\begin{aligned} \mathbf{a}_P \cdot \mathbf{n} &\leq \left(\frac{\omega_x p_x}{a} + \frac{\omega_y p_y}{b} + \frac{\omega_z p_z}{c} \right)^2 - (\omega_x^2 + \omega_y^2 + \omega_z^2) \\ &= (\boldsymbol{\omega} \cdot \mathbf{A}^{1/2} \cdot \mathbf{p})^2 - \omega^2 \leq 0, \end{aligned} \quad (164)$$

the last inequality holds since $(\mathbf{A}^{1/2} \cdot \mathbf{p})^2 = \mathbf{p} \cdot \mathbf{A} \cdot \mathbf{p} = 1$, and so $\mathbf{A}^{1/2} \cdot \mathbf{p}$ is a unit vector.